Forschungszentrum Karlsruhe

in der Helmholtz-Gemeinschaft

Wissenschaftliche Berichte

FZKA 6826

MHD-features of the Main Service and Bypass Pump in the MEGAPIE Design

R. Stieglitz

Institut für Kern- und Energietechnik

Programm Kernfusion

Forschungszentrum Karlsruhe GmbH, Karlsruhe

2003

Impressum der Print-Ausgabe:

Als Manuskript gedruckt

Forschungszentrum Karlsruhe GmbH
Postfach 3640, 76021 Karlsruhe

Mitglied der Hermann von Helmholtz-Gemeinschaft
Deutscher Forschungszentren (HGF)

ISSN 0947-8620

Summary

Within the **Mega**Watt **Pi**lot **E**xperiment (MEGAPIE) to be conducted at the **P**aul-**S**cherrer **I**nstitute (PSI) the feasibility of a lead-bismuth alloy cooled target for spallation purposes will be demonstrated. Such types of liquid metal cooled targets are under consideration for various concepts of **a**ccelerator **d**riven **s**ystems (ADS) aimed to transmute nuclear waste in order to reduce the size of a final repository or to generate fast neutrons for applications like neutron tomography etc. A major component of such targets are the pumps, which are necessary to remove the heat from the highly heat loaded window facing the proton beam generated by the accelarator and transporting the heat through the heat exchangers.

Since the pumps are merely inaccessible for maintenance during operation electro-magnetic pumps without any rotating parts are preferred compared to mechanical devices. Within this report the general performance features of the electro-magnetic tandem pump for the MEGAPIE target being designed and constructed at the Institute of Physics in Riga are reviewed and recalculated using a two-dimensional approach. Additionally the power balance as well as the velocity profile and the operational characteristics are discussed.

The main results of this report are:

a.) Both the main pump as well as the bypass pump will very likely attain the required flow rates. They are in principle capable to reach $27.5m^3/h$ at a pressure head of $0.3bars$ for the main pump and $2.2m^3/h$ at a pressure head of $0.71bars$ for bypass pump. This corresponds to a safety margin of 50%.

b.) The power limiting variable is the input current which should not exceed $37\ Amperes$ for each pump in order to keep the copper winding temperature within acceptable limits.

c.) The overall pump efficiency is extremely weak. It accounts for the main pump to 1.18% and for the bypass unit to only 0.249%. Both is caused by an initially in the design chosen very high slip ratio s which is far above $s=0.5$. The second major reason leading to this weak efficiency is the improper design of the end regions (of in- and outlet), where most of the input power is only spent as eddy loss currents. A proper design here without any change of the pump channel could lead to an order of magnitude higher efficiencies.

d.) The relatively large gap in the main pump causes a pressure variation through the gap in radial direction leading to a non-uniform magnetic induction, which itself leads to a non-uniform velocity profile. This profile has been calculated for nominal conditions. It should be proofed with a computational fluid dynamics code (CFD) if with this profile at the pump outlet the afterwards connected heat exchanger is capable to remove the desired power.

e.) The time scales being given in the report of Platacis and Freibergs (2002) for heating up the pump before filling it with the PbBi do only account for the wall currents and, hence, they are significantly too long. If they would be conducted in the way proposed the pump will very likely be damaged. A more secure way for controlling the up-heating procedure is to use only about 10% of the nominal power and to wait longer times in order to get a more homogeneous temperature distribution in the pump. Therefore, the minimum amount of control thermocouples for each pump are 7. The exact location is given in this report (c.f. fig. 6.1).

f.) In order to avoid misreadings of the pump temperatures by the existing magnetic field and the appearing temperature gradients Copper-Konstantan thermocouples should by used.

g.) A fixation of the iron sheets by means of a mechanical clamping or welding should be used in order to prevent vibrations.

h.) The calculated spaces for thermal expansions in radial of at least $0.85mm$ and axial of at least $0.2mm$ should be existent both on the inductor side **and** the core side due to the different temperatures within the pump. The drawings show spaces but the distances where not given.

i.) Estimates about the response time of the pump to changes in the supply current show a time delay of about $4.89seconds$.

MHD Gesichtspunkte bei der Riga Tandem Pumpe für MEGAPIE

Zusammenfassung

Innerhalb des am PSI in der Schweiz durchzuführenden **Mega**Watt **Pi**lot **E**xperiments (MEGAPIE) wird die Machbarkeit eines flüssigmetallgekühlten Spallationstargets untersucht. Solche Targets werden beispielsweise bei beschleuniger getriebenen Anordnungen (ADS) zur Transmutation langlebiger nuklearer Spaltprodukte betrachtet oder finden bei der Neutronentomographie Verwendung. Ein wichtiges Element eines Targets ist die Pumpe, die zur Wärmeabfuhr des thermisch hoch belasteten Fensters sowie zum Transport des Fluids zum Wärmetauscher benötigt wird. Da diese Pumpen während des Betriebs auf Grund der Strahlenbelastung nicht gewartet werden können werden elektromagnetische Pumpen eingesetzt, die ohne rotierende Elemente auskommen.

In diesem Bericht werden die wesentlichen Eigenschaften der am Institut für Physik in Riga ausgelegten und für das MEGAPIE Target gebauten Tandempumpe nachgerechnet und die wesentlichen kritischen Betriebsparameter beleuchtet. Die Berechnungen basieren auf einem zwei-dimensionalen Ansatz und gelten mit wenigen Abstrichen für alle Arten zylindrischer Induktionspumpen. In einigen weiterführenden Abschnitten wird die Leistungsverteilung, das Geschwindigkeitsprofil am Austritt sowie das Operationsverhalten der Pumpe diskutiert.

Die wesentlichen Ergebnisse der für die MEGAPIE Tandempumpe durchgeführten Berechnungen sind:

a.) Beide, sowohl Haupt- als auch Bypasspumpe werden den angestrebten Durchsatz und die notwendige Druckdifferenz erzeugen und um ca. 50% übertrefffen. Sie sind in der Lage maximal folgende Werte zu erzielen: 1. Hauptpumpe $27.5m^3/h$ bei $0.3bars$ und 2. Bypasspumpe $2.2m^3/h$ bei $0.71bars$

b.) Der leistungslimitierende Parameter ist der zugeführte elektrische Strom, der $37\ Amperes$ nicht übersteigen darf, da sonst die Temperatur in den Kupferwicklungen zu hoch wird.

c.) Die Effektivität der Hauptpumpe beträgt 1.18% und die Bypasspumpe ist mit 0.249% noch schlechter, da in der geometrischen Auslegung von vorneherein ein zu hoher Schlupf gewählt wurde. Ein zweiter wesentlicher Grund ist das nicht angepasste Spulendesign in den Endregionen der Pumpe. Durch die Wahl gleicher Spulenabmessungen überall in der Pumpe wird dort lediglich elektrische Leistung in Wirbelströme und damit ohmsche Wärme umgesetzt. Dort kann die Effektivität um eine Größenordnung gesteigert werden.

d.) Die gewählte große Spaltweite der Hauptpumpe führt zu einem radialen Druckgradienten, mit dem eine radiale Variation des Magnetfeldes einhergeht. Dies führt zu einer radialen Geschwindigkeitsverteilung am Pumpenaustritt, die für den nominalen Betriebspunkt berechnet wurde (Abbildung 7.1). Mit Hilfe eins Fluiddynamikrechencodes sollte überprüft werden ob mit diesem Geschwindigkeitsprofil die gewünschte Wärmeleistung aus dem der Pumpe nachgeschalteten Wärmetauscher abgeführt werden kann.

e.) Die im Bericht von Platacis and Freibergs (2002) angegebenen Zeitskalen für das Aufheizen der Pumpen im ungefüllten Zustand berücksichtigen lediglich die Erwärmung durch die elektrischen Wandströme und nicht die permanent vorhandene Erwärmung durch den Stromfluß in der Wicklung und die Wirbelströme in den Eisenpaketen. Die berechneten Zeitskalen sind daher zu deutlich lang. Werden beide Pumpen bei Nominalbedingungen ca. 30min beheizt, führt dies mit Sicherheit zur deren Zerstörung. Sicherer bei der Aufheizung ist die Nutzung von lediglich 10% der Pumpleistung und längerer Zweiten, um lokalen Überhitzungen zu vermeiden. Zur Temperaturüberwachung während dieser für die Pumpe kritischen Phase wird werden pro Pumpe 7 Thermoelemente vorgeschlagen, deren Positionen der Abbildung 6.1 zu entnehmen sind.

f.) Um Fehler bei der Temperaturmessung durch die vorhandenen Temperaturgradienten und das inhärent existente Magnetfeld zu vermeiden, sollten nicht-ferromagnetische Thermoelemente wie beispielsweise Kupfer-Konstantan Elemente eingesetzt werden.

g.) Zur Vermeidung von Schwingungen insbesondere der Blechpakete sollten diese mechanisch miteinander verbunden werden. Alternativ können sie auch auf der dem Pumpenkanal abgewandten Seite verschweißt werden.

h.) Zum Ausgleich der unterschiedlichen thermischen Ausdehnung der verschiedenen Materialien der Pumpe sollte in axialer Richtung ein Raum von $0.85mm$ und in radialer Richtung von $0.2mm$ vorgesehen werden. Dies gilt sowohl für den Induktor als auch für den Kern.

i.) Die Ansprechzeit der Pumpe auf Leistungsänderungen beträgt ca. $4.89Sekunden$.

TABLE OF CONTENT

1 Introduction

MEGAPIE (Megawatt Pilot Target Experiment) is an initiative launched by Commisariat à l'Energie Atomique, Cadarache (CEA, France) and Forschungszentrum Karlsruhe (Germany) in collaboration with Paul Scherrer Institut (Switzerland), to demonstrate, in an international collaboration, the viability of a liquid lead-bismuth cooled target for spallation facilities at a prototypical size, namely a proton beam power level of 1*MW*. Such a target is under consideration for various concepts of **a**ccelerator **d**riven **s**ystems (ADS) to be used for the transmutation of nuclear waste such as long living fission products and minor actinides as well as other applications like neutron tomography etc..

Using liquid metals like lead or lead-bismuth has also the potential of increasing significantly the thermal neutron flux available in the spallation neutron source SINQ for neutron scattering. The SINQ facility being located at the Paul-Scherrer Institute (PSI) in Villigen Switzerland offers a unique opportunity to realize such an experiment with a reasonably small number of new ancillary systems.

The MEGAPIE experiment will be an important ingredient in defining and initiating the next step, a dedicated ADS-quality accelerator plus irradiation oriented target plus (at a later substage) a low power, sub-critical blanket. It is the goal of this experiment to explore the conditions under which such a target system can be licensed, to accrue a design data base for liquid lead-bismuth cooled targets and to gain experience in operating such a system under the conditions of present day accelerator performance. Furthermore, design validation by extensive monitoring of its operational behaviour and post irradiation examination of its components are integral parts of the project. An extensive pre-irradiation R&D program will be carried out in order to maximise the safety of the target and to optimise its layout.

The only accelerator in Europe which has a sufficiently high proton beam power to make the installation of such a target a meaningful experiment is the ring cyclotron at PSI with 590 MeV proton energy and a continuous current of 1.8 mA, being in the process of an upgrade to 2 mA. It is used for a large range of scientific research tools, the most prominent one is the spallation neutron source (SINQ) with its large number of different user facilities. Furthermore, the very existence of this spallation source with its heavy shielding and complete suite of ancillary systems makes this experiment much more easily affordable.

SINQ is designed as a neutron source mainly for research with extracted beams of thermal and cold neutrons, but hosts also facilities for isotope production and neutron activa-

tion analysis. Except for its different process of releasing the neutrons from matter, it resembles closely a medium flux research reactor for most of its users.

A critical component of the MEGAPIE target experiment is the electro-magnetic pump system, which has been developed at the Institute for Physics in Riga, Latvia. This pump-system is designed as a tandem unit consisting of a main and a bypass pump and is responsible for the circulation of the liquid metal throughout the whole MEGAPIE target. The important task of the main pump is to circulate the fluid via the heat exchanger through the window, while in the bypass pump a jet flow is generated which injects fluid in such a way onto the stagnation point of the window, that an acceptable cooling of this highly heat loaded surface is ensured. The figure 1.1 shows the complete MEGAPIE target experiment design.

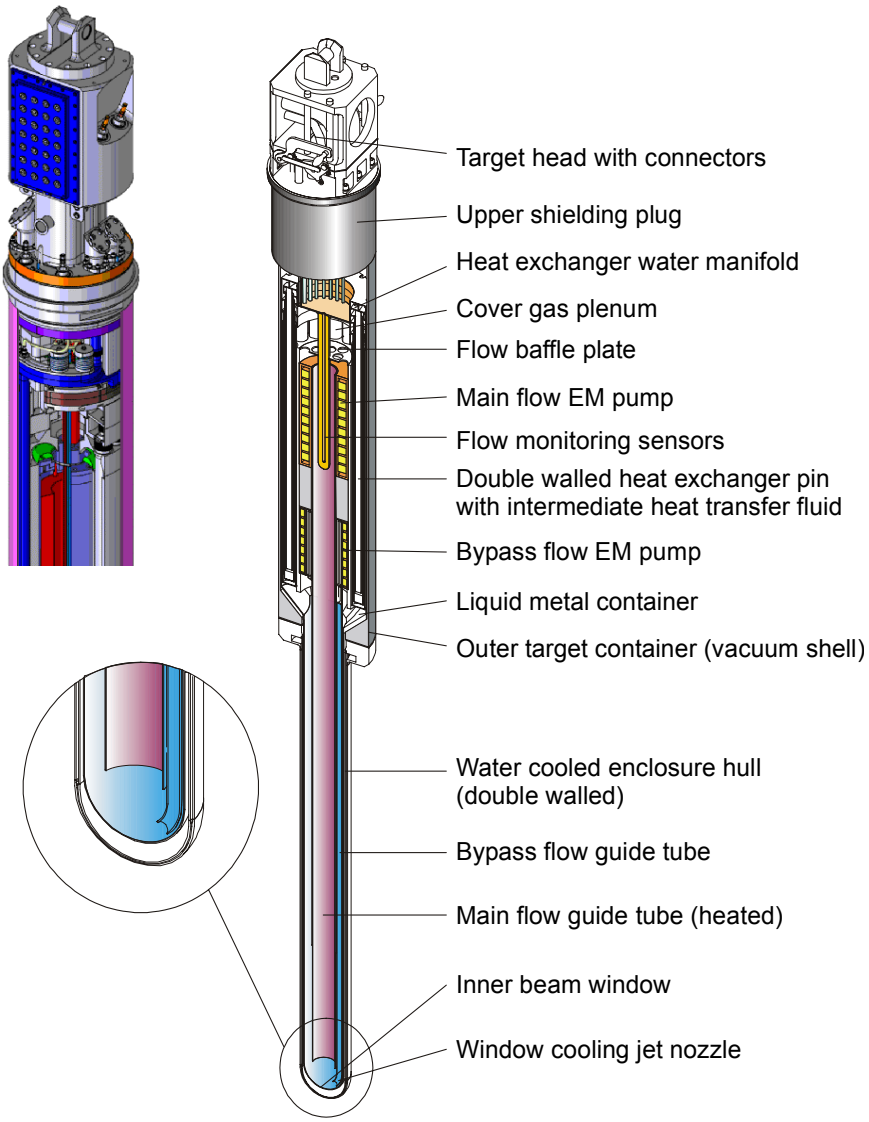

Fig. 1.1: Schematic figure of the MEGAPIE design to be set-up at the PSI in Switzerland.

Within this report the general electro-magnetic pump design requirements are described as well as the principle design of the Riga tandem pump. Further on, some general considerations regarding annular linear induction pumps are drawn before the main design equations are deduced. Based on these design equations the nominal operating point of the pump is recalculated together with the efficiency and other electro-magnetic parameters relevant for the following power balance of the pump in section 5. Also some proposal for a performance increase are given and critical temperature monitoring positions are identified. The velocity profile at the pump outlet is calculated in section 6 before in section 7 the technical design as well as the operation characteristics is discussed. Finally the main results are summarized.

2 Electro-magnetic pump design requirements

The lead-bismuth pump developed by the Institute of Physics of Latvia for the SINQ target at the Paul-Scherrer Institute (PSI) in Switzerland should show at certain nuclear radiation resistance as well as an operation temperature range from 250°C to 480°C. Moreover, it should be nearly maintenance free since a direct access during operation is impossible. A level of maintenance freeness in terms of seals and degradation of the structural material by rotating parts within the liquid metal is offered e.g. by electromagnetic pumps. In this inductor systems a wall normal travelling magnetic field is applied to the duct containing the liquid metal. This travelling field induces within the liquid a potential gradient driving an electric current *j*. The interaction of the electric current with the applied magnetic field produces a Lorentz force thrusting the fluid within the duct. A pump effect can only be achieved if a phase delay Δt between the magnetic field B and the electric current j exists. Thus, an electromagnetic pump acts like an asynchronous motor and the maximum fluid velocity within the duct is always limited to a velocity slower than the travelling magnetic field wave. A sketch of such a pump type is shown in figure 2.1.

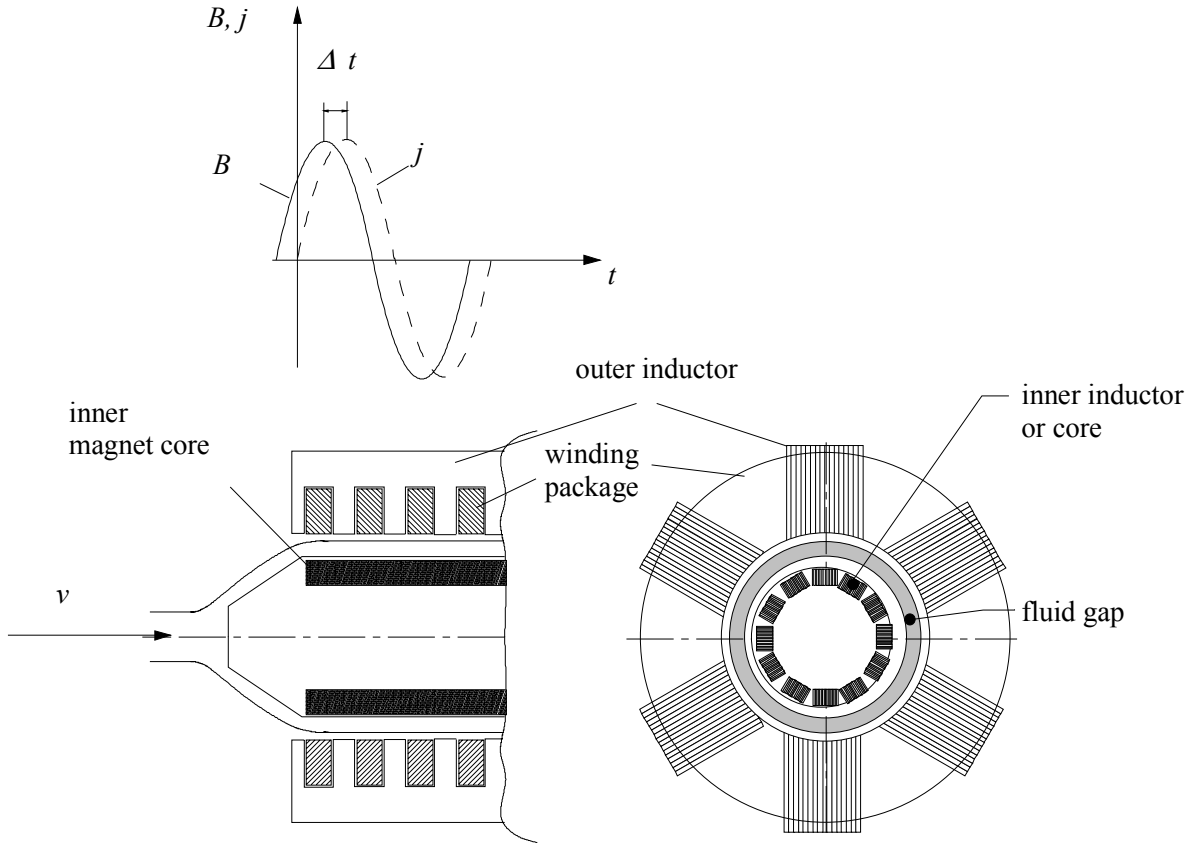

Fig. 2.1: Sketch of the operation principle of an electro-magnetic induction pump on the basis of a cylindrical pump (ALIP).

Annular **l**inear **i**nduction **p**umps (ALIP´s) are more oftenly used than flat linear induction pumps since they are to the first order independent of the electric wetting of the fluid adjacent steel walls. The electric currents close ring like within the fluid gap as shown schematically in figure 2.2. Due to these ring currents the efficiency of ALIPs is significantly higher than for flat devices, but, as all induction pumps they own numerous types of losses, which generally restricts the overall efficiency to values drastically below mechanical pumps. A list of the losses appearing in ALIP´s is given on the right side of figure 2.2.

Within this report we recalculate the pump using a 2D model including to some extend the in- and outlet effects, which leads to the in homogeneity of the magnetic field there. The magnetic field decay towards the non-magnetic environment leads to the production of eddy currents producing Lorentz-forces opposing the desired pump effects. Hence, they do not only contribute to an additional ohmic heating of the fluid but also to a decreased pump performance.

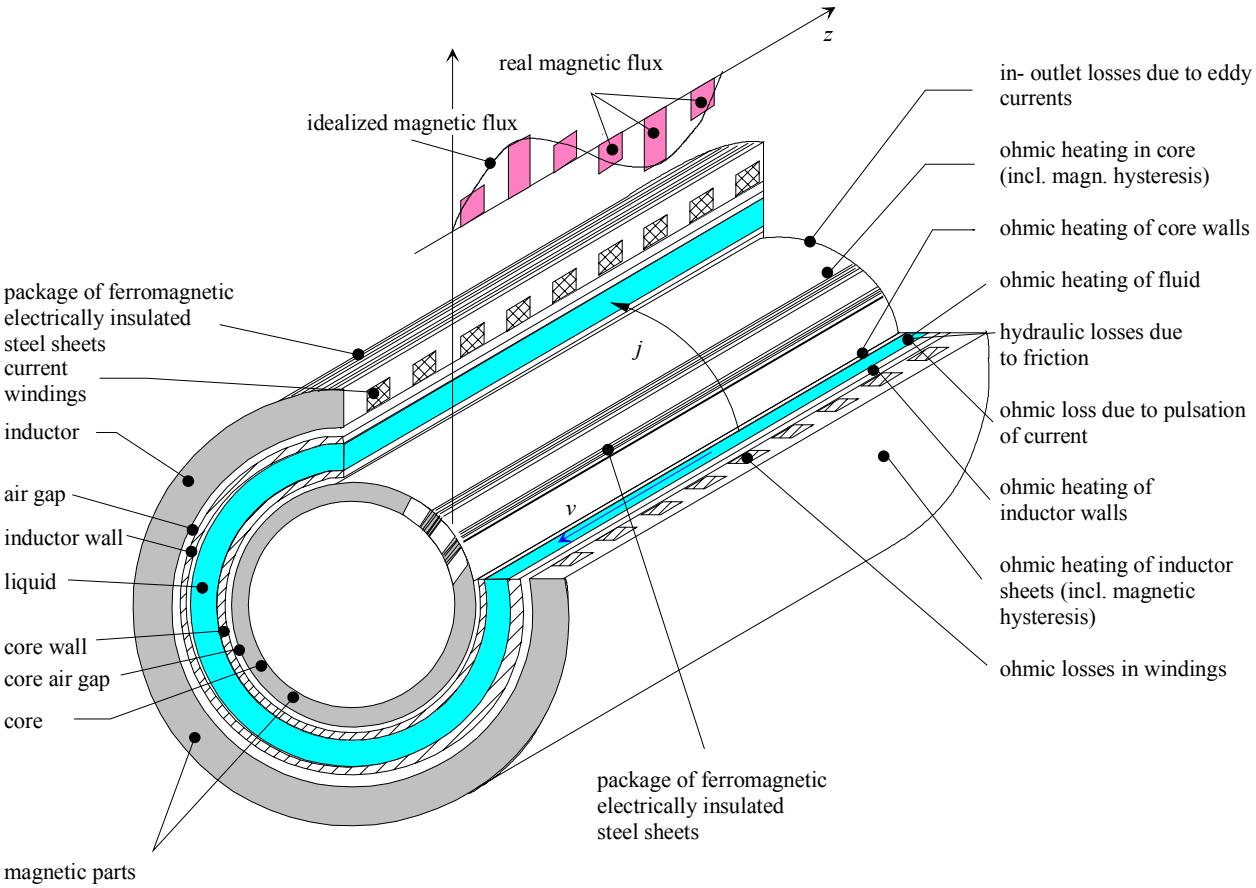

Fig. 2.2: Terminology of the parts being used in an ALIP. Sketch of the generation of the magnetic flux by the windings and a list of the losses appearing in an electromagnetic pump.

3 Mean Parameters of the Pump

The Megapie target pump system is given by two pumps being arranged in series. One pump the main service pump is providing the main flow towards an annular gap and a second pump is delivering the flow rate necessary for the cooling of the stagnation point in the centre of the hemisphere of the beam window. A principle sketch of the pump is shown in figure 3.1.

The design parameters of the constructed bypass pump which is given by the pump manufacturers are displayed in table 3.1.

Parameters	main pump	bypass pump
Δp [Pas 10^5]	0.2	0.5
flow rate Q [m^3/h]	18	1.26
electric Power [kW]	8.2	6.8
active Power [kW]	9.8	8.14
current I [A]	30.3	30.1
current density j [A/mm^2]	6	6
potential ϕ [V]	108	90
induction in Passive core B [T]	1.2	1.14
temperature T_{op} [°C]	480	320

Table 3.1: Power features of the designed MEGAPIE Tandem pump.

Each of the pumps is designed as a 3 pole unit fed by a conventional 50 Hz power supply. The geometric dimensions of both pump units are given in table 3.2.

Design	Main Pump	Bypass pump
effective pump length L [m]	0.36	0.38
liquid metal gap a [mm]	15	5
inner diameter of flow channel d_i [mm]	92	135
outer diameter of flow channel d_a [mm]	122	145
mean diameter of flow channel d_m [mm]	107	140
wall thickness inductor δ_t [mm]	1.5	1.5
wall thickness core δ_t [mm]	1.5	1.5
air gap core inductor δ_{air} [mm]	0.5	0.5

Table 3.2: Design parameters of the designed MEGAPIE Tandem pump.

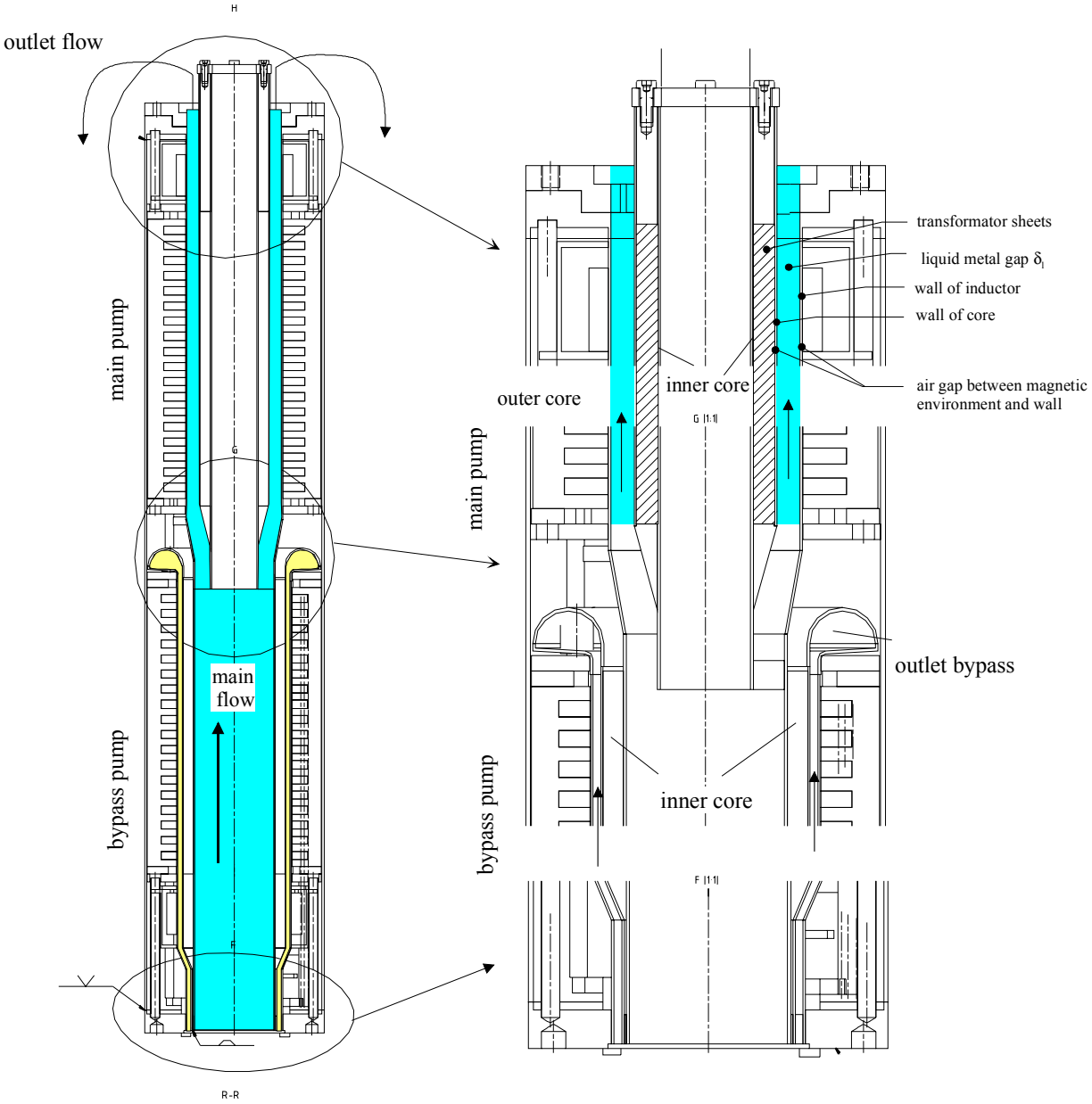

Fig. 3.1: Principle sketch of the tandem pump developed at the Institute for Physics (IP) in Riga for the MEGAPIE target.

4 Some simple electromagnetic considerations

As stated in the introduction Annular linear induction pumps (ALIP´s) are in principle electric asynchronous motors. Hence, some general considerations to this type of motors can be applied to the present Tandem pump design.

We define the following variables which are used in the design, namely:

a.) the wavelength λ,
b.) the mean fluid velocity v_f,
c.) the mean magnetic field velocity v_B
d.) the magnetic slip s and finally
e.) the effective real efficiency η

The latter one includes in this type of approximation the losses appearing at the in- and outlet of the pump.

Using the general equations for asynchronous machines, see e.g. Beitz and Küttner (1986) we obtain the relations 4.1a-e. These relations are uniquely given to asynchronous machines and do not only apply specifically to induction pumps.

In the closed derivation of the mean equations of the design of induction pumps, which is explicitly given in section 5 we finally end with them again.

$$\begin{aligned} \lambda &= \frac{L}{\text{number of poles}}; \\ v_f &= \frac{\text{Flow rate}}{\text{Area of fluid in the gap}}; \\ v_B &= \lambda \cdot f; \\ s &= \frac{\left(v_B - v_f\right)}{v_B}; \\ \eta &= \left(1-s\right)\left(\frac{s}{1+s}\right). \end{aligned} \qquad (4.1a\text{-}e)$$

Using these simple relations and not knowing anything about the induction pump we arrive with the given design parameters of the induction pump at the values displayed in table 4.1.

design unit	main pump	bypass pump
wave length λ [mm]	120	126.67
mean fluid velocity v_f [m/s]	0.992	0.159
mean magnetic field velocity v_B [m/s]	6	6.33
slip ratio s [/]	0.835	0.975
effective real efficiency η [%]	7.52	1.24

Table 4.1: Calculated induction features of the MEGAPIE tandem pump.

For both pump parts of the Tandem pump the slip is rather high and consequently the net efficiency is very low. If we plot the efficiency η of an ALIP-pump as a function of the slip s the diagram in figure 4.1 is obtained.

The efficiency η especially of the bypass pump is inherently low, which is caused by the chosen design. This yields mainly from the very low fluid velocity within the liquid metal gap compared to that of the travelling magnetic field. Thus, most of the power of the bypass pump is transferred as ohmic heating into fluid and the blind power in the coils. Keeping this design a significant increase of the efficiency performance of the bypass pump can only be achieved by a reduction of the power supply frequency or more simply spoken a reduction of the magnetic field v_B velocity. Although the slip s is close to one the operational stability of the bypass pump can be considered as satisfactory in the steady state mode (see e.g. B. Laporte 1980). Only at very low flow rates, if e.g. the pump is started up, instabilities can be expected.

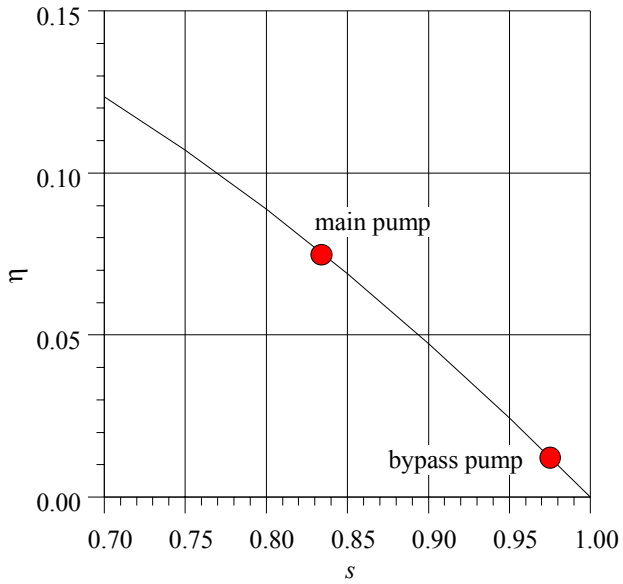

Fig.4.1: Calculated effective efficiency η of the main pump and the bypass pump considering an asynchronous machine as a function of the slip s.

5 Design equations for linear induction pumps

5.1 Ideal linear induction pump

Consider an element of the dimension dx, dy and dz as shown in figure 5.1, where the current density is j_y and the induction is H_x. Equating forces acting on such an element in direction z we obtain a force balance between Lorentz forces (j_y H_x) and pressure forces which is given by equation 5.1.

$$\frac{\partial p}{\partial z} = j_y H_x, \tag{5.1}$$

where p denotes the pressure.

There are similar expressions for the x- and y-components of the pressure at the position (x,y,z). The total pressure developed in a pump of the effective Length L is then given by

$$p_Z = \int_{z=0}^{z=L} j_y H_x \, dz. \tag{5.2}$$

If the pressure is uniform across the tube in the x- and y-direction the gross output power P_0 is given by equation 5.3

$$P_0 = p_z \cdot (v \cdot a \cdot b). \tag{5.3}$$

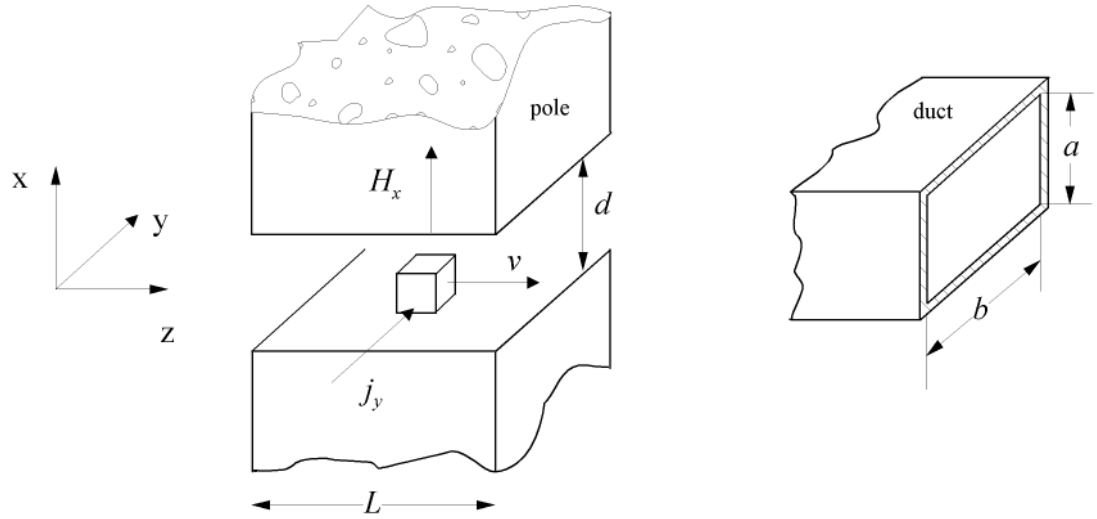

Fig. 5.1: Coordinate system and quantities being used in the pump analysis.

And finally the ohmic loss P_{Ohm} oftenly referred in other papers as Joulean losses (see e.g. Moreau 1980) in the fluid, again assuming uniformity, is

$$P_{Ohm} = \frac{(a \cdot b)}{\sigma} \int_{z=0}^{z=L} j_y^2 \, dz, \tag{5.4}$$

where σ is the specific electric conductivity of the fluid in $A/(Vm)$.

These expressions are basic to all forms of electromagnetic pumps. Other losses in addition to the ohmic heating of the fluid P_{Ohm} is the hydraulic friction loss P_{hydr}, the winding loss P_W, losses in the tube walls P_{tube}, eddy current losses at in- outlet, core losses and so on. In addition, there can be another substantial and perhaps unexpected loss as we will see later.

The design equations for the ideal forms of annular inductions pumps will be considered together by assuming the pump to be flat and of infinite width in y-direction or the electric current flow direction, as indicated in figure 5.2.

A strip of finite width b of this infinite extent corresponds to the mean circumference d_m of the annular gap in the ALIP. Only the x-component of H and the y-component of the current j will be assumed here to exist. The relation between the current density in the fluid j_f, in the tube walls j_t the field H, the core flux Φ per unit length, the magnetizing ampere-turns $\partial NI_m/\partial z$ and the induced voltage per turn ϕ_f/N are derived as follows.

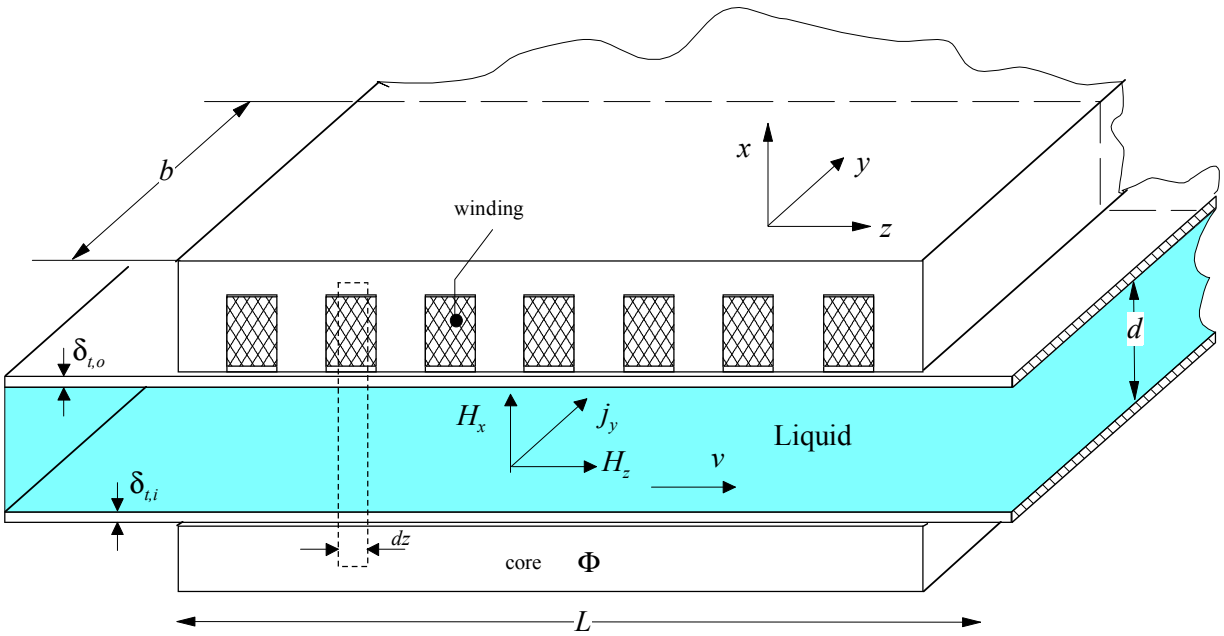

Fig. 5.2: General arrangement and quantities involved in the analysis of a linear induction pump.

Since flux lines are continuous one can write

$$\Phi_Z - \Phi_0 = \int_0^z b\, H\, dz \;\text{ or }\; H = \frac{1}{b}\frac{\partial \Phi}{\partial z}. \tag{5.5}$$

Faradays law yields

$$\frac{10^8 b}{\sigma} j_f = -\frac{d\Phi}{dt} = -\left(\frac{\partial \Phi}{\partial t} + v\frac{\partial \Phi}{\partial z}\right). \tag{5.6}$$

The electric current density in the tube walls j_t is simply derived from j_f by replacing σ with σ_t and putting the velocity v, $v=0$. By applying Amperes law to the circuit of width dz which is shown dashed in figure 5.2 we obtain equation 5.7

$$\left[H - \left(H + \frac{\partial H}{\partial z}\, dz\right)\right] d = \frac{4\pi}{10}\partial N\, I_m. \tag{5.7}$$

and hence we get

$$\frac{\partial N\, I_m}{\partial z} = -\frac{10\,d}{4\pi}\frac{\partial H}{\partial z} = \quad -\frac{10\,d}{4\pi\, b}\frac{\partial^2 \Phi}{\partial z^2}. \tag{5.8}$$

The voltage (or potential difference) per turn induced ϕ_i in the winding is given by

$$\frac{\phi_i}{N} = \frac{1}{10^8}\frac{\partial \Phi}{\partial t}. \tag{5.9}$$

If the flux is assumed to be of the form $\Phi=\Phi_0 \cos(\omega t - \psi)$, as in the induction motor, where $\psi=2\pi z/\lambda$, then we get from relation 5.5

$$H = H_P \sin(\omega t - \psi) \text{ where } H_P = \left(\frac{2\pi}{\lambda b}\right)\Phi. \tag{5.10}$$

Similarly using equations 5.6-5.9 expressions for j_f, j_t $\partial NI_m/\partial z$ and ϕ_i/N can be derived.

$$j_f = \frac{\sigma s v_B}{10^8} H_P \sin(\omega t - \psi), \text{ where } H_P = \left(\frac{2\pi}{\lambda b}\right)\Phi .$$

$$\frac{\partial NI_m}{\partial z} = \frac{5d}{\lambda} H_P \cos(\omega t - \psi)$$

$$j_t = \frac{\sigma_t v_B}{10^8} H_P \sin(\omega t - \psi) \qquad (5.11a\text{-}d)$$

$$\frac{\phi_i}{N} = \frac{v_B b}{10^8} H_P \sin(\omega t - \psi)$$

If these are substituted in equations 5.1 to 5.4 expressions can be deduced for the pump pressure p, the gross power output P_0, and the ohmic losses P_{Ohm} in the fluid and the tube wall P_{tube}.

For P_0 and P_{Ohm} the results are:

$$P_0 = P_\lambda s(1-s) \text{ and } P_{Ohm} = P_\lambda s^2 \text{ where } P_\lambda = \frac{v_B^2}{2\cdot 10^{16}} a b \sigma \lambda H_p^2. \qquad (5.12)$$

An immediate result of the calculation is the ideal efficiency η_i, which is defined by $\eta_i = P_0/(P_0+P_{Ohm}) = (1-s)$. The equations of the ideal case are of limited validity for reasons now to be given and in fact only apply to the mid-section of a linear induction pump.

5.2 End effects in the linear induction pump

It was assumed tacitly in the previous section that the flux Φ is of the form $\Phi_0 \cos(\omega t - \psi)$ over the length L of the pump, $0<z<L$, and the fact that it is zero everywhere outside these limits is ignored. If the effect of the discontinuities of the ends are now considered it is evident from the equations 5.5 and 5.8 that infinities are produced in H and $\partial NI_m/\partial z$ which are not possible to realize in practice. Therefore, assuming the other limiting condition that the magnetizing current distribution $\partial NI_m/\partial z$ is of $\cos(\omega t - \psi)$ form over the length of the pump and is zero outside. For consistency with previous expressions say

$$\frac{\partial NI_m}{\partial z} = \frac{5d}{\lambda} H_P \cos(\omega t - \psi) \quad . \qquad (5.13)$$

The field and flux can be obtained by integrating twice according to equations 5.5 and 5.8. If the boundary conditions are inserted, namely $\Phi_0 = \Phi_{2n\pi} = 0$, then we obtain the following equations.

$$H = H_P \sin(\omega t - \psi) \quad ;$$
$$\Phi = \Phi_0 \left[\cos(\omega t - \psi) - \cos(\omega t)\right]. \qquad (5.14)$$

It will be seen that H and $\partial NI_m/\partial z$ are as before but Φ is different, being supplemented by the pulsating term $\cos(\omega t)$. A repetition of the calculation of power output P_0, and ohmic losses P_{Ohm} and efficiency η_i leads to

$$P_0 = P_\lambda \, s\,(1-s);$$
$$P_{Ohm} = P_\lambda \,\left(1+s^2\right) \qquad (5.15a\text{-}c)$$
$$\eta_i = (1\text{-}s)\cdot\left(\frac{s}{1+s}\right) \quad \text{again with } P_\lambda = \frac{v_B^2}{2\cdot 10^{16}}\, a\, b\, \sigma\, \lambda\, H_p^2.$$

Comparing equations 5.12 with 5.15 shows that the effect of the pulsating component of the flux is to add a pulsating component of the current in the liquid metal, which performs no useful work but increases the ohmic losses by a factor $(1+s^2)/s^2$ and lowers the efficiency by a factor $s/(1+s)$. For example, at a slip of 50%, where the maximum power can be achieved, the ideal efficiency is lowered from 50% to 16.7%. It is evident that these effects are much too large to be tolerated in power conversion systems.

The tandem pump developed in Riga has no optimised set of windings so that the overall efficiency of this pump remains at the low value given in equations 5.15. which yields for the main pump to an efficiency of 7.52% and for the bypass pump of only 1.24%. This quite bad situation in both types of pumps not only affects the efficiency. The too abrupt change of magnetized material towards the non-magnetized environment leads to an overheating of the end winding coils. Hence, these end winding coils, both at inlet ***and*** outlet have to be instrumented in order to prevent a malfunction of the pump or even its destruction. This type of instrumentation is most important for the case where no fluid is in the pump and the travelling magnetic field is used as a heating device for the channel walls. There, all eddy currents are imposed in the structural material and from the electro-magnetic point of view the highest heat density into the structural material is released closed to the end windings.

A dramatic optimisation of the pump performance could be realized if the windings at the in and outlet are graded, in order to get a smoother magnetic flux distribution and thus smaller leakage currents. Although this has been not performed in the Riga design, the author wants to show how this could be realized.

Of course, grading the magnetic core flux over the entire length of the pump leads to the highest efficiency. In case of the Riga pump, which is a rather compact unit this would lead to a design in which each of the 18 windings would be different.

However, the efficiency of the pump would increase to a value of 17.58%. For the bypass

pump the efficiency increase would be more dramatic. Here, the overall efficiency would be 6% at the slip chosen in the present design. Although the grading of the whole core flux is very laborious it shows what potential the pump designers have to optimise such a unit.

A much simpler way to reduce the end losses is to grade the winding over the end sections and leave the mid region uniform. This leads to a simpler arrangement. As an example the winding for the two wavelength at the inlet and outlet could be designed to make the flux over that region to be of the form

$$\Phi = -\frac{1}{2}\Phi_0 \left(1-\cos\psi\right)\cos\left(\omega t-\psi\right). \tag{5.16}$$

Another method is to force the field to be of the form

$$H = \frac{1}{2}H_P \sin\left(\omega t-\psi\right). \tag{5.17}$$

over one pole at each end and the normal form $H_P \sin(\omega t-\psi)$ over the central region. It is easy to show that under these conditions also the flux at the boundary between the end and middle sections (i.e. at $z=\lambda/2$) is of the form $\Phi \cos(\omega t)$ which is the required boundary condition for the middle section and allows the flux to be there of the ideal form $\Phi \cos(\omega t-\psi)$. The expressions for Φ, H, j_f, j_t, $\partial NI_m/\partial z$, $\phi i/N$, P_0, P_{Ohm} and P_{tube} applicable to the end sections can be derived as before. The results are shown in Appendix B, where they can be compared with the results for the ideal case which are given in equation 5.10-5.12.

5.3 Winding design

The total current in the winding includes the magnetizing component $\partial NI_m/\partial z$ already derived and components which cancel the magnetic effects of the current in the liquid and the tube walls by transformer action. The liquid metal current component is $\partial NI_m/\partial z = - j_f a$ and the tube wall current component is given by $-(k_{t1}/s)\, j_f a$. Thus, the ideal distribution of winding current is the vector sum

$$\frac{\partial NI_T}{\partial z} = \frac{\partial NI_M}{\partial z} + \frac{\partial NI_f}{\partial z}\left(1+\frac{k_{t1}}{s}\right). \tag{5.18}$$

For a three phase winding with m coils (or bars) per phase and per pole and one coil (or bar) per slot the total coil current-turns at the position z are

$$NI_T = \frac{\pi}{3}\int_{z-\lambda/12m}^{z+\lambda/12m} \frac{\partial NI_T}{\partial z}\quad dz. \tag{5.19}$$

The factor $\pi/3$ is inserted to give agreement with the analysis of a 3-phase winding and would tend to unity as the number of phases is increased. For the mid section coils equation 5.19 can be written

$$NI_T = \frac{\lambda}{6\, m\, k_d}\left(\frac{\partial NI_T}{\partial z}\right), \tag{5.20}$$

where k_d has the same form as the winding distribution factor that is $k_d = (1/2m)\sin(30°/m)$. The voltage per turn required to excite the coil is

$$\frac{\phi}{N} = \left(\frac{\partial \Phi}{\partial t}\right)_z + \left(NI_T\right)_z\left(\frac{Z}{N^2}\right), \tag{5.21}$$

where Z is the coil impedance (leakage reactance and resistance) calculated as in other electrical machines. The equations 5.18, 5.19 and 5.21 can be applied when designing the coils for both mid and end sections by substituting the appropriate equations of the section §5.1 and §5.3. Calculation of the coil Ampere-turns by the method of equation 5.19 is unorthodox but is suggested since it works equally to end and mid section coils.

5.4 Flux penetration in the induction pump

It is often desirable to employ a large channel width a in a large pump, but it leads to a large value of a/λ, since λ increases only little as the size of the pump is increased. This is because the slip s tends to decrease with size, and although the permissible fluid velocity v_f increases, the synchronous velocity $v_B = v_f/(1-s)$ remains virtually unchanged. Thus, if the frequency is constant $\lambda = v_B/f$ is also virtually independent of the size of the pump. The use of a large value of a/λ is liable to create difficulties due to the limited flux penetration in the gap. So it is necessary to examine these effects.

So far, it has been assumed that the field crosses the gap perpendicularly so that the H_y- and H_z–components are absent. The assumption that H_y is zero is reasonable but it is definitely inappropriate to assume H_z is zero; this is equivalent to ignoring flux penetration effects or, on other words, the reactive impedance to current flow in the liquid metal. A more accurate picture of the field in the gap shows H_x increasing as the winding is approached, and H_x also increasing from zero at the core to an appreciable value on the winding side of the gap. The field variation within the liquid alters the pressure distribution, making p_z low on the core side and also introducing a component p_x, due to the interaction of j_y and H_z. This in turn makes the fluid velocity v_z vary across the gap and introduces a v_x–component. An exact calculation of these effects is complicated for a laminar flow and it is impossible for turbulent flows, which appear in almost all technical applications, because magnetohydrodynamic ef-

fects modify the turbulence structure and thus an isotropic turbulent diffusivity can not be assumed. Nevertheless, useful results can be obtained assuming the H_z–component of the field to be present in addition to the H_x–component, the velocity uniform of value v_f and the v_x–component to be absent. Assume, therefore, that the liquid velocity v_f is constant, and that the components of H and j exist in the following form:

$$H_x = H_1(x)\exp\left[i\omega\left(t-\frac{z}{v_B}\right)\right];$$
$$H_z = H_2(x)\exp\left[i\omega\left(t-\frac{z}{v_B}\right)\right]; \qquad \text{(5.22a-c)}$$
$$j_y = J(x)\exp\left[i\omega\left(t-\frac{z}{v_B}\right)\right].$$

Under these conditions Maxwells first and second equations,

$$rot\, H = \frac{4\pi}{10} j \quad \text{and} \quad rot\; j = -\frac{\sigma}{10^8}\frac{\partial \Phi}{\partial t}; \qquad \text{(5.23a, b)}$$

may be written as

$$\frac{\partial H_x}{\partial z} - \frac{\partial H_z}{\partial x} = \frac{4\pi}{10} j_y;$$
$$\frac{10^8}{\sigma}\frac{\partial j_y}{\partial z} = -\frac{\partial H_x}{\partial t} - v_f \frac{\partial H_x}{\partial z}; \qquad \text{(5.24a-c)}$$
$$\frac{10^8}{\sigma}\frac{\partial j_y}{\partial x} = -\frac{\partial H_z}{\partial t} - v_f \frac{\partial H_z}{\partial z}.$$

Substituting eqs. 5.22 in 5.24 and solving for H_1 and H_2 one obtains

$$\frac{\partial^2 H_1}{\partial x^2} = \gamma^2 H_1, \frac{\partial^2 H_2}{\partial x^2} = \gamma^2 H_2,$$
$$\frac{\partial H_1}{\partial x} = \frac{2\pi i}{\lambda} H_2 \quad , \quad j = \frac{\sigma s v_B}{10^8} H_1 \qquad \text{(5.25a-d)}$$
$$\text{with } \gamma = \frac{2\pi}{\lambda}\sqrt{1+ih} \quad \text{and} \quad h = \frac{2}{10^9}\sigma s \lambda v_B.$$

The boundary conditions which must be satisfied are $H_2 = 0$ and from 5.25c, d

$$\frac{dH_1}{dx} = 0 \quad \text{at} \quad x = 0. \qquad \text{(5.26a)}$$

This assumes in the arrangement of figure 5.2 that the core is of infinite permeability and cannot sustain the field H_2 parallel to its surface. For the second boundary condition many forms are possible. If the winding current is known, on can write

$$H_2 = H_{2a} \text{ and } \frac{dH_1}{\partial x} = \frac{2\pi i}{\lambda} H_{2a} \text{ at } x = a \quad , \qquad \text{with } H_{2a} = \left(\frac{4\pi}{10}\right)\frac{dNI_T}{dz} \quad . \tag{5.26b, c}$$

The latter expression is a reasonable approximation in most cases. If the supply voltage is known, or more accurately the induced voltage ϕ_i which is the supply voltage less the voltage drop in the winding impedance, then the following relation holds.

$$H_1 = H_a \text{ at } x = a \text{ where } \frac{\phi_i}{N} = \frac{v_B b\, i\, H_a}{10^8} \quad . \tag{5.27}$$

A further possibility is to suppose that the mean field across the gap is known

$$\frac{1}{a}\int_{x=0}^{x=a} H_1\, dx = H_p \, , \tag{5.28}$$

using the same symbol H_P as before but denoting now the peak value in time of the mean gap field. Any of the equations 5.26-5.28 can be employed in solving equations 5.25; all have relative merits but equation 5.28 appears to be most convenient when comparisons with previous expressions are to be made. This boundary condition will be employed together with the one of equation 5.26. The solution reduces then to

$$\frac{H_1}{H_P} = \frac{\gamma a \quad \cosh(\gamma x)}{\sinh(\gamma a)} . \tag{5.29}$$

It is useful for design purposes to evaluate

$$\frac{H_a}{H_P} = \frac{\gamma a}{\tanh(\gamma a)} = \left|\frac{H_a}{H_P}\right| \exp(i\varsigma). \tag{5.30}$$

This finally reduces to

$$\left|\frac{H_a}{H_P}\right| = \left(\cosh M + \cos N_1\right)\sqrt{\frac{M^2 + N_1^{\,2}}{\left(\sinh M\right)^2 + \left(\sin N_1\right)^2}}\;;$$

$$\text{and}\quad \varsigma = \frac{1}{\arctan\left(\dfrac{N_1}{M}\right)} - \frac{1}{\arctan\left(\dfrac{\sin N_1}{\sinh M}\right)}\quad ; \tag{5.31}$$

$$\text{where } M = \frac{4\pi a}{\lambda}\sqrt{\frac{\sqrt{1+h^2}+1}{2}} \quad \text{and} \quad N_1 = \frac{4\pi a}{\lambda}\sqrt{\frac{\sqrt{1+h^2}-1}{2}}.$$

It is also desirable to know the pressure difference on either side of the channel. This can be done by substituting equations 5.25c and d and equation 5.29 into relation 5.2. The integration finally leads to

$$\frac{p_a}{p_0} = \frac{\cosh M + \cos N_1}{2}. \tag{5.32}$$

The gross power output P_0 based on a pressure averaged across the gap and in time as well as the ohmic loss in the fluid P_{Ohm} are given by the following relations:

$$P_0 = P_\lambda\, s\left(1-s\right)\cdot\zeta \quad \text{and} \quad P_{Ohm} = P_\lambda\, s^2\cdot\zeta;$$

$$\text{with } P_\lambda = \frac{v_B^2}{2\cdot 10^{16}}\, a\, b\, \sigma\, \lambda\, H_p^2 \quad \text{and} \quad \zeta = \frac{\left(M^2 + N_1^2\right)\left(\dfrac{\sinh M}{M} + \dfrac{\sin N_1}{N_1}\right)}{4\left(\cosh M - \cos N_1\right)} \tag{5.33}$$

From these relations one gets for the configuration of the Riga tandem pump the following parameter sets for the final design calculation.

Design	Main pump	Bypass pump
gap/wavelength ratio a/λ	0.125	0.039
H parameter	1.01 10^{-3}	1.317 10^{-3}
pressure variation in gap height $\frac{p_a}{p_0}$	1.76	1.0638
max. induction variation across the gap $\frac{H_a}{H_P}$	1.55	1.02

Table 5.1: Parameter values for the Riga tandem pump for the two dimensional calculation.

5.5 Final design recalculation of the Riga Tandem pump

In the previous sections the basic steps for the calculation of an ALIP have been derived. With the given design parameters we now can calculate the operational parameters of the pump.

Since the internal heating of the coil windings determines the achievable pressure head, the coils have to be designed in such a way that an optimal connection between the coils for a given pressure head leads to a minimum electrical current density. For an ideal ALIP (Annular Linear Induction Pump) assuming no end effects and fine displaced coils equation 5.34 holds.

$$\frac{J^2}{\Delta p} = \frac{\left(\frac{2\pi a}{\mu_0 f \lambda^2}\right)^2 + \left(\delta_t \sigma_t + \left(1 - \frac{v_f}{\lambda f}\right)\delta_f \sigma_f\right)^2}{\sigma_f L \frac{\left(1 - \frac{v_f}{\lambda f}\right)}{\lambda f}} \tag{5.34}$$

Herein, δ is the whole distance over which the induction is applied, namely $\delta = 2\delta_t + 2\delta_{air} + a$ and σ is the specific electric conductivity of the walls or the fluid, which are characterized by the indices "*t*" and "*f*". For the stainless steel the specific electric conductivity σ is almost constant and given by $\sigma = 1.33 \cdot 10^6\ A/(Vm)$. The thermohydraulic data for lead-bismuth are taken from Yefimov et al. (1996). The magnetic permeability of vacuum μ_0 is given by $\mu_0 = 4\ \pi\ 10^{-7}\ As/(Vm)$.

Inserting the design parameters (or geometrical extensions) of section §3 into equation 5.34 we obtain the electric current to be supplied by windings to the duct as a function of the wavelength λ at a given frequency *f* of the travelling magnetic field. The figures 5.3a and 5.3b show the necessary current density per meter for both parts of the Riga tandem pump.

Using this relation we get for the bypass pump a minimum current supply to the duct of $J = 8974\ A/m$ and for the main pump $J = 14982\ A/m$. The slip *s* to be given by the design calculates to $s = 0.9748$ for the bypass pump and $s = 0.835$ for the main pump, respectively.

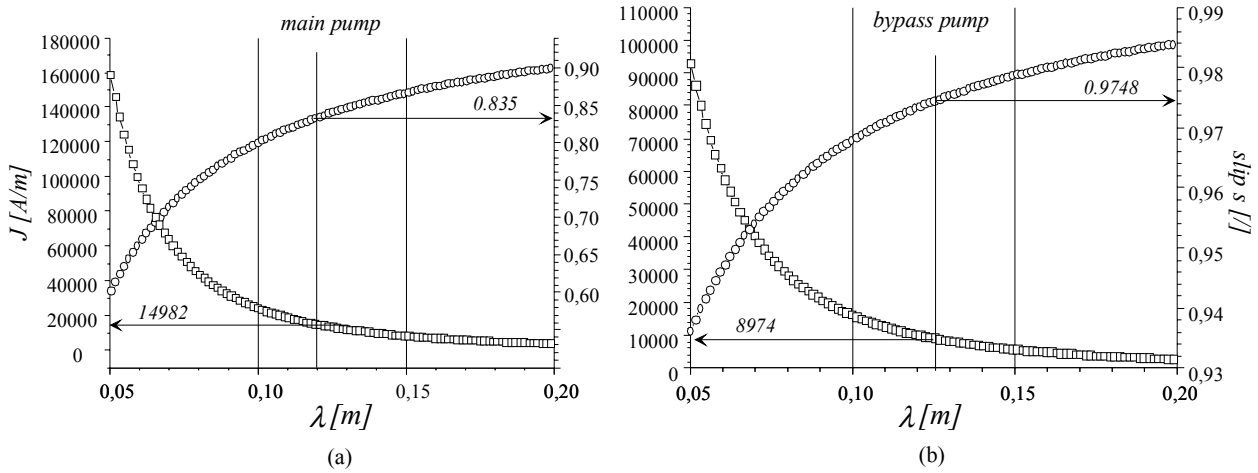

Fig. 5.3: Electric current density *J [A/m]* required to attain the desired pressure head as a function of the wavelength λ for the main pump (a) and the bypass pump of the Riga tandem pump.

The weak efficiency of both pumps (bypass: $\eta_i=1.25\%$, main $\eta_i=7.5\%$) will result in a high ohmic heating of the duct and the fluid within the pumping channel. Since the thermal heat conductivity of $Pb^{45}Bi^{55}$ is as weak as that of stainless steel, thermal problems may arise. Choosing a lower slip also offers the capability to realize a higher pressure head of the pump if demanded by the user, e.g. by reducing the frequency of the power supply. By choosing a high slip the design is more or less fixed and modifications without drastic changes of the pump construction are hardly possible.

Hence, in order to improve the efficiencies to more acceptable values for the main pump the following measures could be taken

a.) In order to reduce the slip the gap size could be reduced. A reduction of the gap size from 10 to 5 mm would reduce the required current density from *14982A/m* to *11673A/m*. The slip would be *s=0.763* and the efficiency would increase to $\eta_i=10.25\%$. Moreover, a smaller gap size has the advantage of a lower pressure variation over the gap since the magnetic field in the gap is higher and more homogeneous and, thus, it leads to a higher pump stability.

b.) The frequency could be reduced to e.g. *f=30Hz*. This leads to a higher current density required to attain the preferred pressure head. The effect on slip and efficiency, however is simultaneous to measure a.).

c.) Finally, the best solution would be a mixture of both a reduction of the gap size *a* to $5mm$ and a reduction of the frequency to $f=40Hz$, then the current density would be $16983A/m$, the slip $s=0.7039$ and the efficiency $\eta_i=12.23\%$.

In case of the bypass pump the situation is much more difficult, since the gap width is already very small and from a hydraulic and manufacturing point of view it can not be significantly reduced. Nevertheless, in order to get an increased performance with a gap size of $2.5mm$ and a feeding frequence of the field of $30Hz$ a current supply of $14306A/m$, would be required leading to a slip $s=0.918$ and a efficiency $\eta_i=4.0\%$.

Based on the calculations of the pump design with equations 5.34 we can calculate the electric potential in the windings Φ to obtain the pressure head desired in the following way:

$$\frac{\phi_i^2}{\Delta p} = \frac{(\pi d_m)^2 \lambda f}{\sigma L\left(1-\frac{v_f}{\lambda f}\right)}. \tag{5.35}$$

The peak magnetic induction H_P directly at the coils can then be calculated. The magnetic inductions reads to:

$$H_p = \frac{\phi_i}{(\lambda f)\pi d_m}. \tag{5.36}$$

Finally, the peak magnetic field is amplified by packages of ferromagnetic sheets, which own a magnetic permeability μ being significantly larger than unity. In order to calculate the effective magnetic permeability leading to the amplification of the induction we have to integrate the room filling of the material in the active part (, which means the height of the windings, the inner core and the space in between which is the area to be pumped). The result has to be averaged over the whole volume being treated. Finally, a multiplication of the cubic root of this value with the peak induction gives the peak magnetic field to be obtained in the arrangement.

Assuming an effective magnetic permeability of the iron plates of about $\mu=5000$ at $400°C$, which is obtained for the german TRAFOPERM of Vakuumschmelze Hanau (, which is similar to the used POZH700), we get for the main pump an effective permeability of $\mu=17.29$ and for the bypass pump of $\mu=9.71167$.

The real current density J_{real} is given by the geometrical design of the slots and the windings, which are displayed in table 5.2 and can be calculated using equation 5.37.

$$J_{real} = \sqrt[3]{\mu}\,\frac{n_{\text{current turns}} \cdot n_{slots} \cdot J}{n_{\text{Poles}} \cdot L}\,. \tag{5.37}$$

Design	Main Pump	Bypass pump
number of slots	18	18
current turns per slot	24	16
number of poles	3	3
slot width [mm]	11	11

Table 5.2: Electric connection of inductor of the MEGAPIE tandem pump.

Using relation 5.37 for the main pump the real current density is $J_{real}=31340A/m$ (required was $J=14982A/m$) and for the bypass pump $J_{real}=16320A/m$ (required was $J=8974A/m$). The real current densities in the pump are significantly higher than those required to attain the postulated pressure head. Even if we consider in the 2D case massive inlet and outlet effects using a vector potential formulation as being used by Blake (1956) or Leboucher (1992) the required applied current density increases by 25%. In case of the main pump this does not lead to any problems since the security margin is more than a factor of 2. The margin for the bypass pump is thereby lower, but nevertheless even in the worst case the bypass pump will very likely attain the named pressure head and the designed flow rate.

Summarizing now all results obtained for the electro-magnetic performance of the designed Riga tandem pump we obtain the table 5.3. In this table all mean parameters of the pump are shown. The values shown here form the basis for the power balance calculations in the following section

Formulation	relation	Eq.nr.	Unit	Main pump	Bypass pump
Wave length λ	$\lambda = \frac{L}{\text{number of poles}};$	4.1a	*m*	*0.12*	*0.12667*
Fluid velocity v_f	$v_f = \frac{\text{Flow rate}}{\text{Area of fluid in the gap}}$	4.1b	*m/s*	*0.992*	*0.159*
Magnetic field velocity v_B	$v_B = \lambda \cdot f$	4.1c	*m/s*	*6*	*6.33*
Slip ratio s	$s = \frac{(v_B - v_f)}{v_B}$	4.1d	/	*0.835*	*0.975*
Electric potential ϕ_i	$\frac{\phi_i^2}{\Delta p} = \frac{(\pi d_m)^2 \lambda f}{\sigma L\left(1 - \frac{v_f}{\lambda f}\right)}.$	5.35	*V*	*0.2315*	*0.43957*
Peak induction by coils	$H_p = \frac{\phi_i}{(\lambda f)\pi d_m}$	5.36	*Tesla*	*0.1148*	*0.1579*
Effective mean magnetic permeability μ	μ		/	*17.29*	*9.7117*
Max. magnetic field at the coils B_{max}	$B_{\max} = \mu \cdot H_p$		*Tesla*	*1.9845*	*1.5333*
Induction variation along gap height	$\left\|\frac{H_a}{H_p}\right\| = (\cosh M + \cos N)\sqrt{\frac{M^2 + N^2}{(\sinh M)^2 + (\sin N)^2}}$	5.31a		*1.55*	*1.02*
Power factor P_λ	$P_\lambda = \frac{v_B^2}{2 \cdot 10^{16}} a\, b\, \sigma\, \lambda\, H_p^2$	5.12	*W*	*120.87*	*119.2*
Power output	$P_0 = P_\lambda\, s(1 - s)$	5.15a	*W*	*16.65*	*2.9055*
Pump efficiency η_i	$\eta_i = (1\text{-}s)\left(\frac{s}{1+s}\right)$	5.15c	/	*7.52*	*1.24*
Real current density J_{real}	$J_{real} = \sqrt[3]{\mu}\, \frac{n_{\text{current turns}} \cdot n_{slots}}{n_{\text{Poles}} \cdot L}$	5.37	*A/m*	*31340*	*16320*
Required current density J	$\frac{J^2}{\Delta p} = \frac{\left(\frac{2\pi a}{\mu_0 f \lambda^2}\right)^2 + \left(\delta_i \sigma_i + \left(1 - \frac{v_f}{\lambda f}\right)\delta_f \sigma_f\right)^2}{\sigma_f L \frac{\left(1 - \frac{v_f}{\lambda f}\right)}{\lambda f}}$	5.34	*A/m*	*14982*	*8974*
Pressure variation in gap height	$\frac{p_a}{p_0} = \frac{\cosh M + \cos N}{2}.$	5.32	/	*1.76*	*1.0638*
h-factor	$h = \frac{2}{10^9} \sigma\, s\, \lambda\, v_B$	5.25d	/	*1.01 10^{-3}*	*1.33 10^{-3}*
Nominal mean operation temperature T_{op}			°C	*320*	*280*
Specific electric conductivity at operation temparature $\sigma(T=T_{op})$	$\sigma(T) = 10^6(0.95266 - 3.456 \cdot 10^{-4} T).$	*B	*A/(Vm)*	*8.421 10^5*	*8.558 10^5*

Table 5.3. Electro-magnetic performance of the designed Riga tandem pump..
*B see Appendix B.

6 Power balance of the Riga Tandem Pump

The electric power input in the system using a conventional 3-phase power supply with the potential ϕ and the current I yields at the operation point of the pump to an electric gross power input of:

$$P_{Input} = 3 \cdot \phi \cdot I \cdot \cos\varphi \quad , \tag{6.1}$$

where $\varphi=30°$ is the phase shift between voltage and current.

The total hydraulic pumping power is given by

$$P_{hydraulic} = \Delta p \cdot v_f \cdot \frac{\pi}{4}\left(d_a^2 - d_i^2\right) \quad , \tag{6.2}$$

In order to determine the hydraulic losses in the pump the hydraulic Reynolds number has to be calculated using equation 6.3.

$$Re = \frac{v_f \cdot d_h}{\nu} \quad , \tag{6.3}$$

with d_h the hydraulic diameter (d_h=d_a-d_i) and the kinematic viscosity ν. The loss factor ξ_F can be calculated using the Blasius relation given in equation 6.4:

$$\xi_F = \frac{0.3164}{\sqrt[4]{Re}} \quad . \tag{6.4a}$$

The pressure drop $\Delta p_{viscous}$ through the whole pumping duct can be obtained by.

$$\Delta p_{viscous} = \frac{\rho}{2} \cdot v_f^2 \cdot L\left(\xi_F + \xi_{i,o}\right) \quad , \tag{6.4b}$$

Here, the hydraulic pressure drop coefficients $\xi_{i,o}$ are calculated using form relations collected in the book of Zierep& Bühler (1991). These relations yield for the main pump a form factor of $\xi_{i,o} = 0.82$ for the main pump and for the bypass pump of $\xi_{i,o} = 0.82$, respectively. Knowing the pressure drop in the duct the power loss due to viscous forces $P_{viscous}$ can be easily evaluated using relation 6.4c.

$$P_{viscous} = \Delta p_{viscous} \cdot v_f \cdot \frac{\pi}{4}\left(d_a^2 - d_i^2\right) \quad , \tag{6.4c}$$

The ohmic losses P_{ohm} within the fluid can then be calculated using equation 5.15 and the following derivation in chapter 5 by the following equations 6.5

$$\begin{aligned} P_\lambda &= v_B^2 \frac{\left(d_a - d_i\right)}{2} \cdot \frac{\pi}{10} \cdot d_m \ \sigma \lambda \cdot \overline{B^2}, \\ P_{Ohm} &= P_\lambda \left(1 + s^2\right) \quad , \end{aligned} \tag{6.5a,b}$$

where $\overline{B}$ is the mean magnetic field strength in the gap. Assuming a magnetic field distribution behaving as a potential function the mean magnetic field in the gap of the main pump is $\overline{B} = 1.01 Tesla$, where it is in the bypass pump $\overline{B} = 1.31 Tesla$.

However, additional ohmic losses appear due the electric current flow in the tube of short-cut core of the pump $P_{t,s}$ and the tube walls adjacent to the coils P_t. The current circulating in the tube walls J_t can be estimated assuming ideal electrical contact at the fluid-wall interface using the following relations:

$$\begin{aligned} J_t &= \left(\lambda \cdot f\right) \sigma_t \, \overline{B} \left(\delta_t \cdot L\right) \quad ; \quad R_t = \frac{1}{\sigma_t} \cdot \frac{2}{\pi\left(d_a + \delta_t\right)} \quad ; \\ P_t &= R_t \cdot J_t^2 \quad , \end{aligned} \tag{6.6a-c}$$

where R_t is the wall resistance in Ohm (Ω).

Besides to the direct ohmic heating due to the current flow within the tube walls the ferromagnetic iron sheets within the core of the pump are also "*microwave*" heated. Although the iron sheets are separated from each other by a resistive oxide layer (which is electrically insulating) the electric currents induced into them can circulate throughout the inner core, because the sheets are embedded in the electrically conducting structural material. The appearing currents can hardly be calculated, but assuming an hyperbolic decay of the magnetic induction within the core the flux penetration can be assumed. Consider now steel sheets of a radial extension of 10mm with approximately a similar specific electric conductivity than that of the stainless steel tube we obtain a power input into the magnetic permeable iron sheets of $P_{Iron,S}$=752W for the main pump and $P_{Iron,S} = 428W$ for the bypass pump. In the outer iron sheets the heat released there is of a similar order of magnitude. A calculation based on

a similarity analysis of the active iron volume leads to iron losses in the outer sheets of $P_{Iron,o}$=802W for the main pump and $P_{Iron,o}$=493W for the bypass pump, respectively.

Finally, the current through the copper coils and the connection between the coils cause also an ohmic loss. We consider conservatively a specific electrical conductivity of copper σ_{Cu} at $T=500°C$, i.e. of $\sigma_{Cu} = 4.1\ 10^7 A/(Vm)$. The coils being designed consist of 24 windings per coil in the main pump and 16 in the bypass unit.

First, we calculate the ohmic resistance in the main pump coils. If we assume a fill factor F of the coils of F=0.9, and a tooth depth of $28mm$ the average diameter of the coils is $d_{m,coil}=140mm$. Hence, each of the main pump coils owns then a length of $10.55m$. Conservatively assessed we assume including the connections a coil length of $l_{coil}=11.73m$. The total resistance R_{wind} in all coils as well as the power released there P_{Coil} is then given by:

$$R_{wind} = \frac{4}{\pi} \frac{l_{coil}}{\sigma_{Cu}\, A_{coil}} \cdot n_{slots}; \qquad P_{wind} = 3 \cdot R_{Coil} \cdot I^2_{\mathrm{sup}ly} \quad , \tag{6.7a,b}$$

where A_{coil} is the current carrying cross section area of the winding. In the Riga pump this cross section is $A_{coil} = 5.37\ 10^{-6} m^2$. Similarly we get for the bypass pump, where the filling factor in the gap is due to the large extensions decreased to $F=0.85$ a coil length of $8m$ and using the filling factor then l_{coil}=9.4m.

Finally, we arrive at the power balance given in table 6.1 for the Riga tandem pump.

From the calculated power balance of the tandem pump we can determine the time threshold, which the pump needs to heat up its channel walls in case of the start-up procedure. In this calculation one has to be extremely careful, because not only the induced wall currents lead to a heating up of the channel walls but also heat conduction through the structural material, since the other heat sources like the ohmic heating in the winding as well as the heating of the iron sheets by eddy currents contribute to a temperature increase on the pump wall.

Description		Unit	Main pump	Power [%]	Bypass pump	Power [%]
Phase shift voltage current	φ	[°]	30		30	
Nominal potential supply	ϕ_i	V	108		90	
Nominal electric current	I	A	30.3		30.1	
Mean operation Temperature	T_{op}	°C	320		280	
Hydraulic Reynolds number	Re	/	$1.65\ 10^5$		$8\ 10^3$	
Blasius friction coefficient	ξ_F	/	0.0157		0.0335	
In- /Oulet friction coefficient	$\xi_{i,o}$	/	0.82		0.86	
Pressure drop due to friction in the pump	Δp_p	Pas	3400		100	
Power factor	P_λ	W	1871.2		1639.4	
Tube current at coil side	$J_{t,Coil}$	A	5402		4728	
Ohmic resistance coil tube	R_{Coil}	Ω	$3.97\ 10^{-6}$		$3.34\ 10^{-6}$	
Tube current at core side	$J_{t,Co}$	A	2755.7		4680	
Ohmic resistance core tube	R_{Core}	Ω	$5.24\ 10^{-6}$		$3.59\ 10^{-6}$	
Ohmic resistance of winding	R_{wind}	Ω	1.22		0.97	
Electric power input	P_{input}	W	8502	100.00	7038.2	100.00
Hydraulic power	P_{hydr}	W	100.4	1.18	17.5	0.25
Viscous fluid heating	P_{vis}	W	17	0.20	3	0.04
Ohm fluid heating by current P_I and field pulsation P_ω	P_I P_ω	W W	1304.6 1871.2	15.34 22.01	1558.5 1639.4	22.14 23.29
Ohm heating tube wall at coils	$P_{t,coil}$	W	115.8	1.37	74.7	1.06
Ohm heating tube wall at core	$P_{t,coe}$	W	39.8	0.47	78.6	1.12
Eddy current heating of iron sheets coil system	$P_{Iron,S}$	W	752	8.84	428	6.08
Eddy current heating of iron sheets core system	$P_{Iron,o}$	W	802	9.43	493	7.00
Ohmic heating of winding	P_{WindS}	W	2809.4	33.04	2636.5	37.46
Miscellaneous losses	P_{WindS}	W	689.8	8.12	109	1.56
Total power	P_{tot}	W	8502	100.00	7038.2	100.00
Overall Pump-efficiency P_{hydr} / P_{input}	η	%		**1.18**		**0.249**

Table 6.1: Power balance diagram of the Riga tandem pump.

In order to get an estimate about the longest time being necessary to heat up the channel wall we suppose the following conditions:

a.) an adiabatic heating up of the channel wall which is caused only by the induced wall currents at nominal operating conditions (I=30A, ϕ=108V)

b.) Neglection of any heat convection through the inertgas.

c.) Neglection of the heat input by the ohmic heating of the windings.

d.) Neglection of the heat input arising from the eddy currents circulating in the iron sheets.

With all these assumptions one can calculate the temporal temperature Δt rise in the wall tubes in seconds per degrees $°C$ using this simple relation.

$$\Delta t = \rho_{SS} \cdot \frac{\pi}{4}\left[(d_a + \delta_t)^2 - d_a^2\right] L \cdot \frac{c_{SS}}{P_{t,coil}} \Delta T \quad , \tag{6.8}$$

where c_{ss} is the heat capacity of stainless steel in $J/(kgK)$ and ρ_{SS} its densitiy in kgm^{-3}. The values for steel are c_{SS}=510$J/(kgK)$ and ρ_{SS}=7853 kgm^{-3}.

If we insert these values into the equation 6.8 and calculate the temperature rise in the coil tube of the main pump we arrive for the temperature rise at a value of $\Delta t/\Delta T$=8.33$s/(°C)$. This means if we would heat up the tube only with this current from $20°C$ to $200°C$ we would need $25minutes$. This corresponds approximately to the value being reported by Freibergs and Platacis 2002 for the main pump (there 27 minutes are calculated). If one would really await this time the winding set would be already been blown (assuming the same adiabatic conditions as for the coil tube wall, with c_{Cu}=390$J/(kgK)$ and ρ_{Cu}=8960 kgm^{-3}). After $25min$ at nominal operating conditions assuming still constant material properties the winding copper temperature would be $922°C$(!!!). This shows that the time constants given in this report should be taken with extreme care.

A detailed calculation of the start-up time is due to the complex geometrical arrangement, the mixed composition of the pump (copper, ferromagnetic iron, stainless steel, electric insulation material, power supply lines, connectors) and the numerous heat transfer processes (volumetric heating by means of inductive heating and ohmic heating, surface heating and

radiation heating due to the different temperature levels of the different materials) hardly feasible and would be more than of speculative nature.

Thus, a rather smooth start-up procedure in the inert gas filled state with maximum 10% of the nominal power is strongly recommended. A detailed instrumentation at the most critical points of the pump can prevent a failure of the Tandem pump. The exact position of the most critical locations within the pump are marked in figure 6.1 for the example of the main pump. At these points the temperature should be continuously been monitored during the start-up and the filling. A similar arrangement should be installed for the bypass pump.

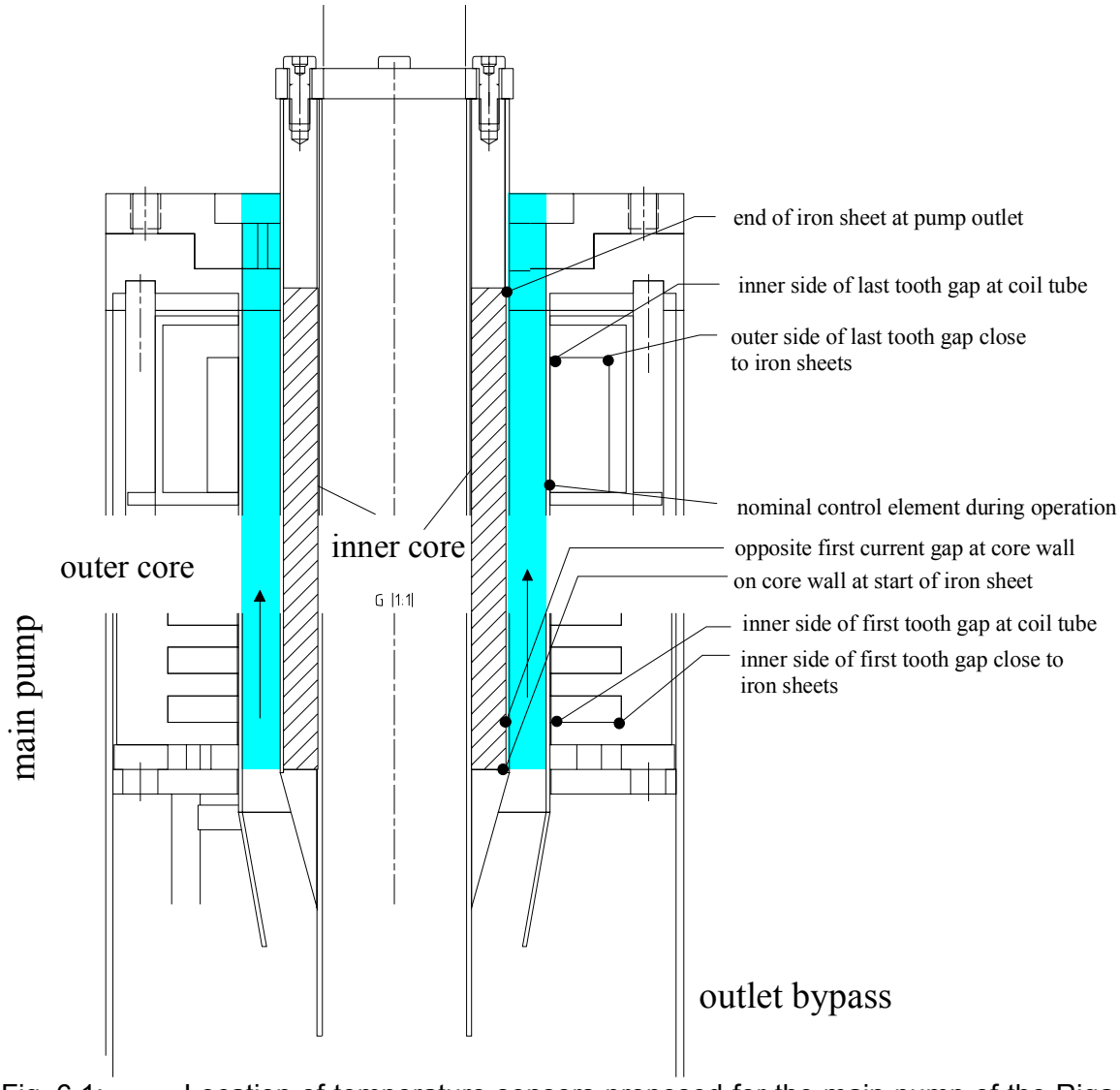

Fig. 6.1: Location of temperature sensors proposed for the main pump of the Riga tandem pump.

7 Velocity field at the Outlet

One crucial question in the past is the velocity field at the outlet of the main pump. The velocity field at the bypass pump is more or less of slug flow type since the mean induction and the pressure gradient over the gap hardly vary.

In order to get a rather rudimentary access to the velocity profile, we assume a two-dimensional MHD flow neglecting the pressure variation in radial direction over the gap.

The Hartmann number Ha (, which weigths the electromagnetic forces versus the viscous ones,) being attained by the induction is given by relation (7.1a) and the composite Stewart number St (, which denotes the electromagnetic forces versus the inertial ones) is given by equation 7.1b.

$$Ha = d_m B\sqrt{\frac{\sigma_f}{\rho \cdot \nu}} \quad ; St = \frac{d_m \sigma B^2}{\rho \nu_f} \tag{6.1a,b}$$

At a temperature of $T=480°C$, and a mean induction (geometrically averaged via $2\pi B(r)\ r\ dr$) of B of $0.85Tesla$ we get a Hartmann number of $Ha=2130$. The Stewart number St determining the influence of inertia forces to electromagnetic forces yields for the outlet a value of $St=5\text{-}6$.

Due to the high Hartmann number the flow is mainly prescribed by the magnetic field distribution. So the velocity profile close to the outlet follows approximately the magnetic field distribution. Considering the interaction parameter St we are in a regime where $St<<Ha^{3/2}$ holds. This means that inertial forces smooth the periodic variations of the electromagnetic forces and thus an axi-symmetric velocity field establishes (see. e.g. Alemany and Moreau 1977).

The velocity profile splits of in a core region and an inertial viscous side layer of the thickness $\delta \sim St^{-1/3}$. The thickness of this side layer is in case of the main pump about $0.5mm$ and the velocity within the constant magnetic field region is usually very small there. At the end of the pump, however, the fluid in the side layer is accelerated due to the potential differences within the pump compared to those outside the pump. The velocities obtained in the side layer immediately after leaving the pump region can reach in case of the main pump $1.82m/s$.

But, due to the small thickness of the side layer they do not contribute significantly to the overall flow rate.

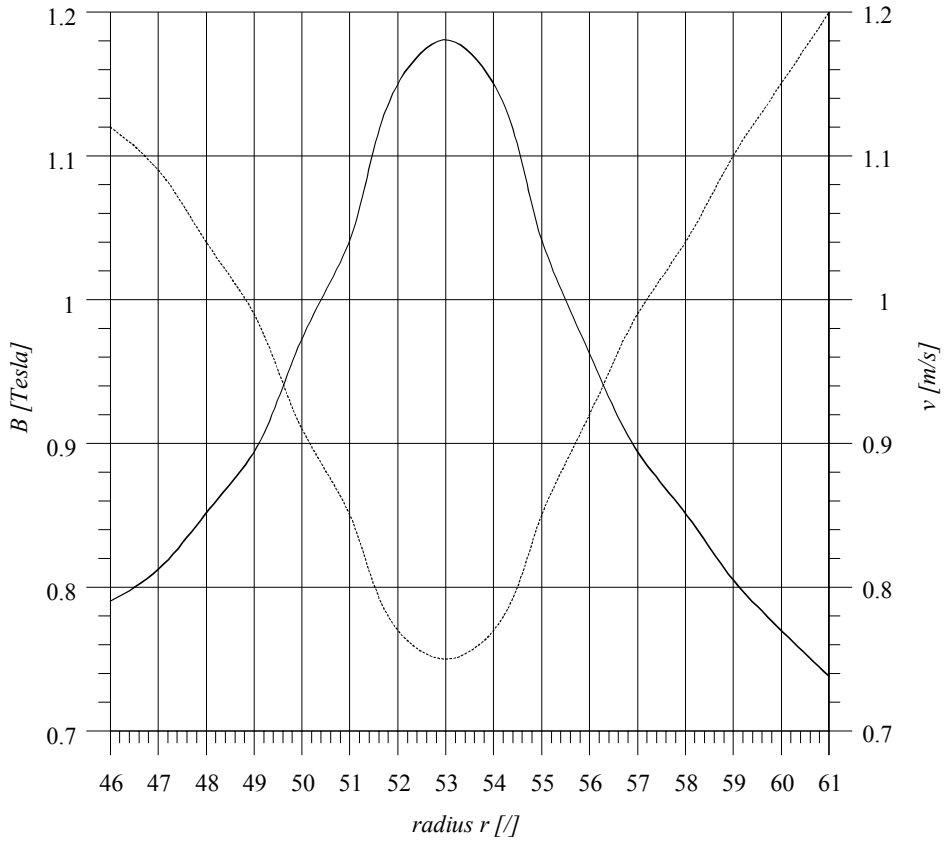

Fig. 7.1: Velocity (——) and magnetic field (– – –) distribution as a function of the radius at the end of the main pump.

8 Technical design, operational characteristics

A design sketch of the main pump of the Riga tandem system is shown in figure 8.1, and the bypass unit is displayed in figure 8.2.

In the inner part of the inductor system steel sheets of highly magnetic permeable iron (here quality *3413*) are pressed into the grooves of an inner tube. This steel package consists of *678* sheets in the main pump (the bypass unit owns *1068* sheets), which are electrically separated from each other by an oxide layer.

From the drawings it is unclear how the individual steel sheets are compressed onto each other. This compression is necessary in order to prevent the packages from oscillations, because the eddy currents induced in the individual sheets cause circumferrential forces tending to pull the sheets away from each other. For the considered power supply of $f=50Hz$ the penetration depth of the currents is about $6mm$, so that the steel sheets of the inductor may even be point welded together at 4 or 5 axial positions. The same procedure can be performed at the inner inductor. This procedure can be used for both the main and the bypass pump.

It is also unclear from the technical drawings how the support structure of the inner core in both pumps looks like. The inner tube should allow a certain thermal expansion not only in axial direction but also in radial direction without any loss of its structural integrity.

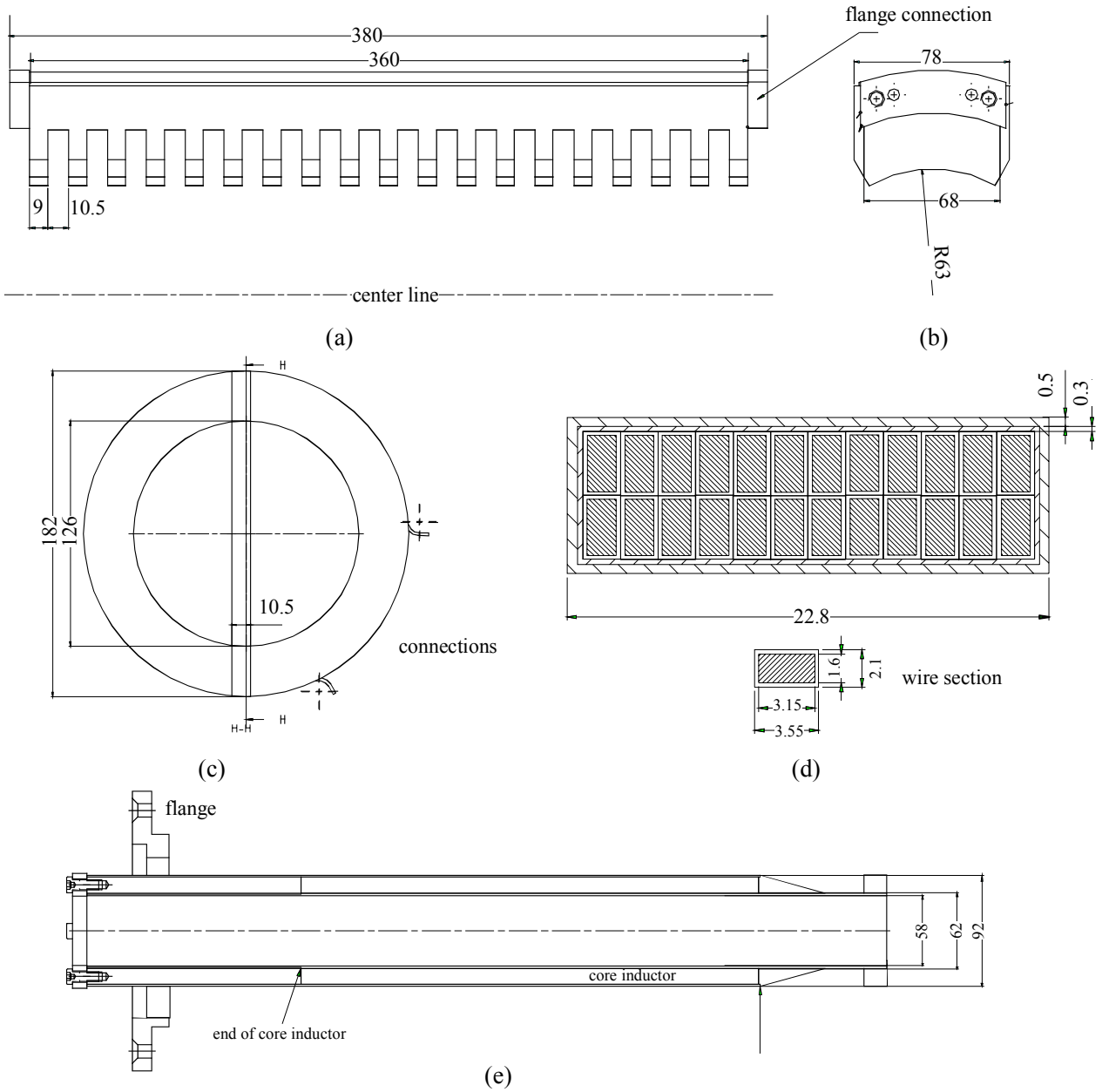

Fig. 8.1: Technical sketch of the main pump of the Riga tandem unit. (a) Iron package consisting of 678 steel sheets. (b) extension of the ferromagnetic iron package. (c) Coil system and its connectors. (d) cross sectional cut through one coil package and wire dimensions. (e) Inner core inductor and its dimensions.

The reason is the higher thermal conductivity of the steel being used compared to the pumped fluid lead-bismuth. This bad heat conductivity of the fluid is responsible for a high temperature within the inductor. The second reason of much higher temperatures in the core is that about *9%* of the pump power in case of the main pump and *7%* in case of the bypass pump is displaced as ohmic heating in the iron sheets. First estimates show that the overheat

compared to the adjacent fluid may be at maximum $125°C$ in the main pump, which is the worst case, since in the main pump the inner inductor is not forced convectively cooled as the one of the bypass pump.

Considering an overheat of $125°C$ the axial thermal expansion of the iron sheets are about $0.85mm$ and the corresponding radial expansion is $0.2mm$.

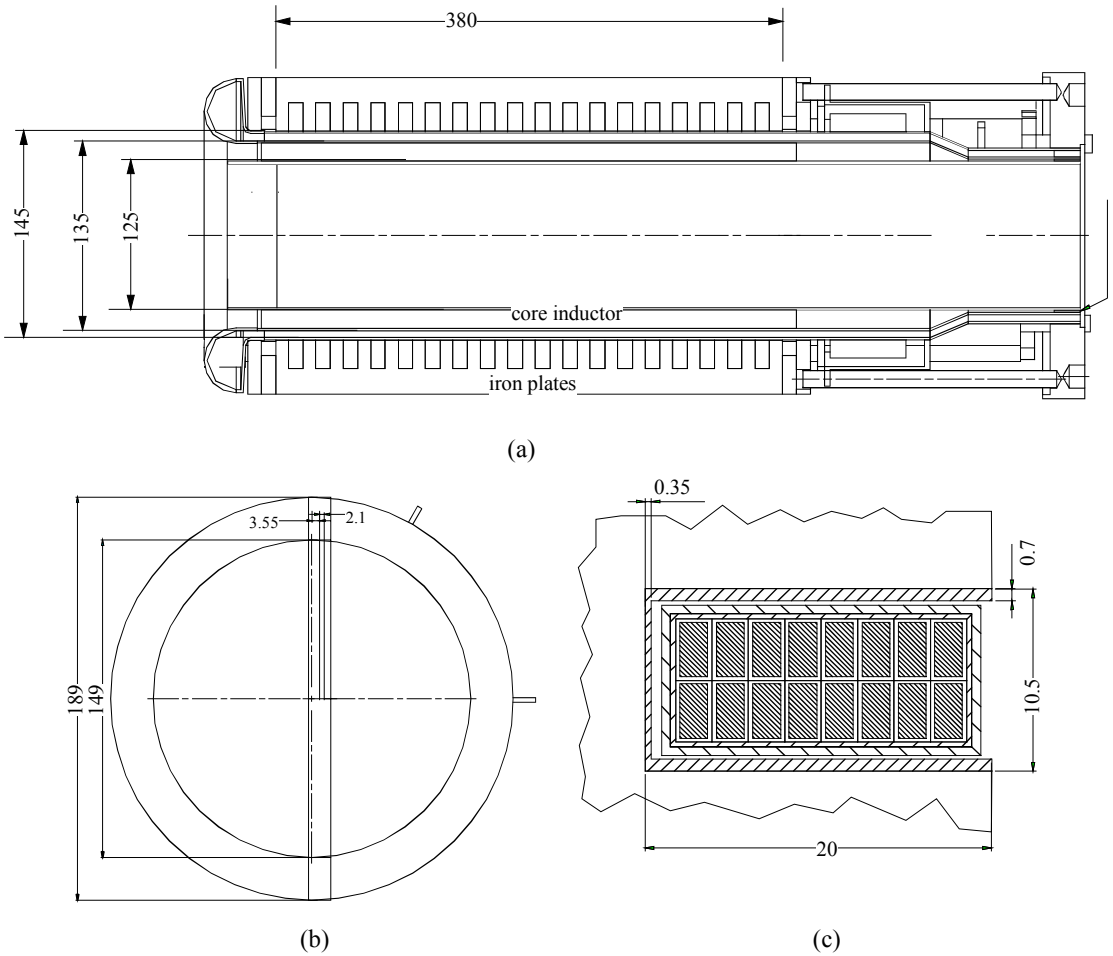

Fig. 8.2: Technical sketch of the bypass pump of the Riga tandem unit. (a) Inductor and inner core, Iron package consisting of 1068 steel sheets. (b) Coil system and its connectors. (c) cross sectional cut through one coil package (wire dimensions are the same as in the main pump).

Since the magnetic fields in induction pumps can reach significant values, thermometry errors can occur due to the Seebeck-effect, the Nernst-Ettingshausen-effect, Galvanomagnetic effects or the Righi-Leduc effect, see Kollie et al. (1977). The misreading due to these effects can be of order $20°C$ up $50°C$. Especially, the most commonly used thermocouple Chromel-Alumel (Ni-NiCr) is affected by this effects. In order to minimize misreadings in controlling the inductor temperatures Copper-Konstantan thermocouples (Cu-CuNi) should be used, because none of there branches is ferromagnetic. They can be used up to temperatures of about $550°C$-$600°C$.

Although the pump is designed in its operation point for the nominal net frequency of $f=50Hz$ a frequency and potential variable supply would be desirable, because at lower frequencies the attainable pressure head and as a consequence the flow rate can be increased. A frequency variable electric pump supply control represents in the context of the MEGAPIE module also a safety feature because if the hydraulic characteristics of the MEGAPIE target is changed and a higher pressure head is required one can use only the magnitude of the electric current as an adjustment screw. (The limiting frequency is given for the case, where the synchronous velocity of the field is approaching nearly the fluid velocity in the duct).

A pump characteristic diagram as a p-V diagram makes no sense in case of the MEGAPIE design since the module has no regulation valves and thus the flow rate as well as the pressure head establishing after a certain time only depends on the electric current being supplied to the duct. Thus, we draw the attainable pressure head Δp and the resulting flow rate Q as a function of the supply current I in figure 8.3.

Generally, for both units of the Riga tandem pump the maximum power output is not determined by the current supply, it is rather given by the height of the ohmic losses in the windings. With increasing current supply the over-temperature in the windings continuously increases leading to increasing thermal expansion and, moreover, to an increasing ohmic resistance in the windings. This increasing resistance (, which is to the first order linear growing with the temperature) leads together with the quadratically in current increasing ohmic loss to unacceptably high over-temperatures.

Thus, if we assume a maximum copper coil temperature of $T=550°C$ and additionally considering only heat conduction towards the surrounding structural materials we arrive for the bypass pump at a maximum acceptable current *I* of approximately $I=37.32A$. Nearly the same limiting current the main pump has it accounts to $I=37.11A$. Nevertheless, the flow rates which will be attained by both pumps will be more than 60% than those required. Of course, the assumption of heat conduction to the environment is rather conservative, but due to the increasing thermal expansion of the windings with temperature the distance of the windings tend to grow away from the inductor wall and the effectiveness of the pump weakens. Thus, it seems to be a reasonable consideration.

Another important question to the operator of the module is how fast the flow rate will change after a change in the electric supply current.

Therefore, in order to get a feeling of the inertia and the time constants to be expected, we assume the MEGAPIE module to have an inventory of $80liters$ of fluid at a mean temperature of $320°C$. In order to accelerate the flow rate in the main pump from zero to nominal flow rate we can use a simple equation of motion using the mass as the inertial part. The maximum start-up time is then $t=4.89seconds$.

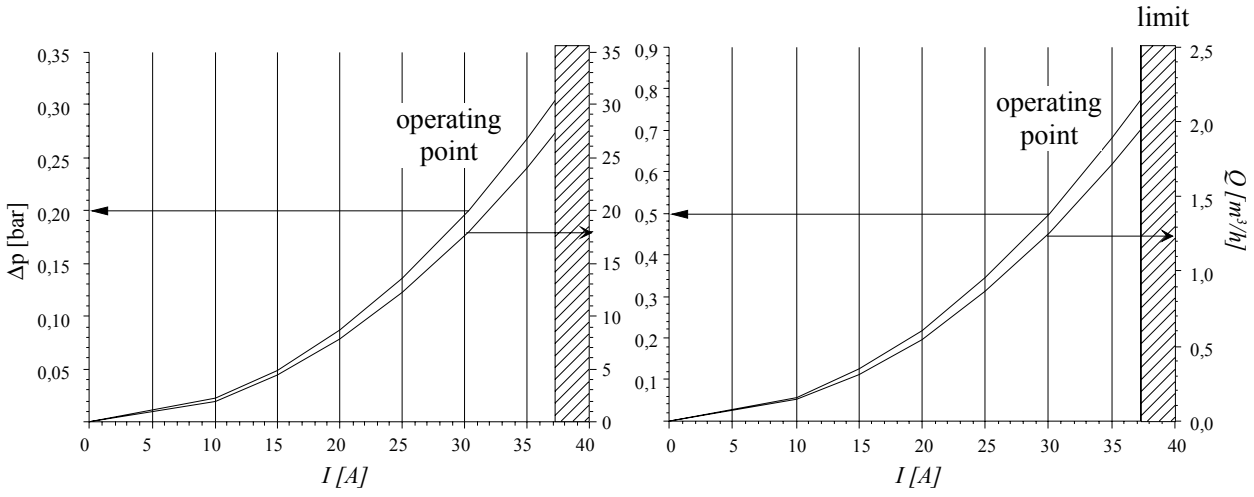

Fig.8.3: Attainable pressure head Δp in bar and related flow rates Q in m^3/h of the main pump (a) and the bypass pump (b) as a function of the supplied current I in *Ampere*.

9 Summary

Within the **Mega**Watt **Pi**lot **E**xperiment (MEGAPIE) to be conducted at the **P**aul-**S**cherrer **I**nstitute (PSI) the feasibility of a lead-bismuth alloy cooled target for spallation purposes will be demonstrated. Such types of liquid metal cooled targets are under consideration for various concepts of **a**ccelerator **d**riven **s**ystems (ADS) aimed to transmute nuclear waste in order to reduce the size of a final repository or to generate fast neutrons for applications like neutron tomography etc. Major components of such targets are the pumps, which are necessary to remove the heat from the highly heat loaded window facing the proton beam of the accelarator and transporting the heat through the heat exchangers.

Since the pumps are merely inaccessible for maintenance during operation electromagnetic pumps without any rotating parts are preferred compared to mechanical devices. Within this report the general performance features of the electro-magnetic tandem pump for the MEGAPIE target being designed and constructed at the Institute of Physics in Riga are reviewed and recalculated using a two-dimensional approach. Additionally the power balance as well as the velocity profile and the operational characteristics are discussed.

The main results of this report are:

a.) Both the main pump as well as the bypass pump will very likely attain the required flow rates. They are in principle capable to reach $27.5m^3/h$ at a pressure head of $0.3bars$ for the main pump and $2.2m^3/h$ at a pressure head of $0.71bars$ for bypass pump. This corresponds to a safety margin of 50%.

b.) The power limiting variable is the input current which should not exceed 37 *Amperes* for each pump in order to keep the copper winding temperature within acceptable limits.

c.) The overall pump efficiency is extremely weak. It accounts for the main pump to 1.18% and for the bypass unit to only 0.249%. Both is caused by a very high slip ratio s being far above $s=0.5$, which was initially chosen in the design. The second major reason leading to this weak efficiency is the improper design of the end regions (of in- and outlet), where most of the input power is only spent as eddy loss currents. A proper design here without any change of the pump channel could lead to an order of magnitude higher efficiencies.

d.) The relatively large gap in the main pump causes a pressure variation through the gap in radial direction leading to a non-uniform magnetic induction, which itself leads to a non-uniform velocity profile. This profile has been calculated for nominal conditions. It should be proofed with a computational fluid dynamics code (CFD) if with this profile at the pump outlet the afterwards connected heat exchanger is capable to remove the desired power.

e.) The time scales being given in the report of Platacis and Freibergs (2002) for heating up the pump before filling it with the PbBi do only account for the wall currents and, hence, they are significantly too long. If they would be conducted in the way proposed the pump will very likely be damaged. A more secure way for controlling the up-heating procedure is to use only about 10% of the nominal power and to wait longer times in order to get a more homogeneous temperature distribution in the pump. Therefore, the minimum amount of control thermocouples for each pump are 7. The exact location is given in this report (c.f. fig. 6.1).

f.) In order to avoid misreadings of the pump temperatures by the existing magnetic field and the appearing temperature gradients Copper-Konstantan thermocouples should by used.

g.) A fixation of the iron sheets by means of a mechanical clamping or welding should be used in order to prevent vibrations.

h.) The calculated spaces for thermal expansions in radial of at least $0.85mm$ and axial of at least $0.2mm$ should be existent both on the inductor side **and** the core side due to the different temperatures within the pump. The drawings show spaces but the distances where not given.

i.) Estimates about the response time of the pump to changes in the supply current show a time delay of about $4.89seconds$.

10 References

Alemany A., Moreau, R., 1977, *Journal de Mechanique Theory and Application*, Vol. **16**, p.635ff.

Beitz, W, Küttner, K.-H., 1986, Dubbel-Taschenbuch des Maschinenbaus, Springer-Verlag, 15th edition; *ISBN 3-540-12418-7*, p. 1211 ff.

Blake, L.R., 1956, Conduction and induction pumps for liquid metals. The Institution of Electrical Engineers. Unwin Brothers Limited Woking and London *UDC 621.313.1.621.88*.

Freibergs, E., Platacis, E. 2002, Electro-magnetic pump system- A detailed design. Institute for Physics Report IPUL 1069.00.00-05.

Imbeni, V. Martini, C., Masini, S., Palombarini, G., 1999, The properties of the eutectic alloys Pb55.5Bi and Pb17Li. ENEA-Report DT-EUB-00001, Part 2.

Kollie, T.G.; Anderson, R.L.; Horton, J.L.; Roberts, M.J. 1977 Large thermocouple thermometry errors caused by magnetic fields; Rev. Science Instrum.; Vol.48; No. 5; pp.501-511.

Laporte, G, 1980 “About specific windings for induction linear motors; *Proc. ICEM*, 1980.

Leboucher, L., 1992, Optimisation des convertisseurs MHD a induction: probleme inverse en electromagnetise. Thesis Univ. Grenoble (in French).

Lyon, R.N. 1952 Liquid metals handbook; Navexos P-733; Second edition.

Yefimov, E.I. 1996 Preconceptional design of a 1MW flow Lead-bismuth target. State Scientific Centre of Russian Federation- Institute of Physics and Power Engineering. Report *No. 35-06/64-1996*

Zierep, J, Bühler, 1991 K. Strömungsmechanik, Springer Verlag, *ISBN 3-540-53827-5*, p. 82ff

11 Appendix A

Thermophysical properties of $Pb^{55}Bi^{45}$

T [°C]	ρ [kg/m^3]	λ [W/(mK)]	$\nu\,10^{-7}$ [m^2/s]	$\sigma\,10^5$ [A/Vm)]	c_p [J/(kgK)]
130	10558.25	11.07	3.006	9.004	150.385
150	10531.17	11.16	2.719	8.943	149.908
200	10462.42	11.66	2.275	8.771	148.715
250	10393.67	12.17	1.971	8.600	147.523
300	10324.92	12.68	1.754	8.428	146.330
350	10255.75	13.19	1.592	8.257	145.138
400	10187.42	13.70	1.467	8.085	143.945
450	10118.25	14.21	1.369	7.914	142.753
500	10049.5	14.72	1.290	7.742	141.560
550	9981.17	15.23	1.225	7.751	140.368
600	9912.42	15.73	1.172	7.399	139.175
700	9774.92	16.75	1.089	7.056	136.790

The thermohydraulic correlations used in the pump calculations are for the

a.) density ρ [kg/m^3] :

$$\rho(T) = 10737 - 1.375 \cdot T \quad \text{with } T \text{ in } [°\text{C}] \quad \text{valid for } 130<T<1000 \tag{A1}$$

b.) specific heat conductivity λ [$W/(mK)$]

$$\lambda(T) = 9.63 + 1.0174 \cdot 10^{-2} \cdot T \quad \text{with } T \text{ in } [°\text{C}] \quad \text{valid for } 130<T<700 \tag{A2}$$

c.) kinematic viscosity $\nu\,10^{-7}$ [m^2/s] :

$$\nu(T) = 4.6635 - 1.675 \cdot 10^{-2} \cdot T + 2.855 \cdot 10^{-5} \cdot T^2 - 1.71 \cdot 10^{-8} \cdot T^3 \quad \text{with } T \text{ in } [°\text{C}]$$

valid for $130<T<700$ (A3)

d.) specific electric conductivity σ 10^5 [$A/(Vm)$] :

$$\sigma(T) = 9.43873 - 3.343 \cdot 10^{-3} \cdot T \quad \text{with } T \text{ in } [°\text{C}]$$

valid for 130<T<500 (A4)

e.) heat capacity c_p [$J/(kg\ K)$] :

$$c_p(T) = 153.4854 - 2.385 \cdot 10^{-2} \cdot T \quad \text{with } T \text{ in } [°\text{C}]$$

valid for 130<T<700 (A5)

The thermo-physical values are taken from Imbeni et al. (1999), Lyon (1952) and Yefimov (1996).

12 Appendix B

Performance increase of ALIP-designs by means of graded end regions

The grading of the in- outlet regions in order to increase the pump performance has been sketched in section 5. The relevant equations with which a grading of the windings could be performed are the equations 5.16 and 5.17, which are lateron referred to as method A and method B. Here again are the named equations:

$$\Phi = -\frac{1}{2}\Phi_0 \left(1-\cos\psi\right)\cos\left(\omega t-\psi\right). \tag{B.1}$$

The method B is to force the travelling magnetic field to be of the form

$$H = \frac{1}{2}H_P \sin\left(\omega t-\psi\right). \tag{B.2}$$

Generally the method A is suitable for small sized ALIP pumps as the Riga one, where the Ohmic loss in the fluid P_{Ohm} is not the predominant one. The method B is oftenly used for split winding ALIP´s where it is convenient and simple to employ in practice as it involves a double layer winding over the mid sections, which naturally leads to a single layer winding over the end poles (, it would be the most preferred option for the bypass pump).

The expressions for Φ, H, j_f, j_t, $\partial NI_m/\partial z, \phi i/N$, P_0, P_{Ohm} and P_{tube} applicable to the end sections can be derived as in section 5 and here only the end results are given.

The calculations leads for method A to

$$\begin{aligned}
\Phi &= -\frac{1}{2}\Phi_0 \left(1-\cos\psi\right)\cos\left(\omega t-\psi\right) \quad ;\\
H &= -\frac{1}{2}H_P \left[\sin\psi\cos\left(\omega t-\psi\right)+\left(1-\cos\psi\right)\sin\left(\omega t-\psi\right)\right] \quad ;\\
J_f &= \frac{\sigma s v_B}{2\cdot 10^8}H_P\left[\left(1-\cos\psi\right)\sin\left(\omega t-\psi\right)-\frac{1-s}{s}\sin\psi\cos\left(\omega t-\psi\right)\right] \quad ;\\
J_t &= \frac{\sigma_t v_B}{2\cdot 10^8}H_P \left(1-\cos\psi\right)\sin\left(\omega t-\psi\right) \quad ;\\
\frac{\partial NI_m}{\partial z} &= \frac{5d}{\lambda}H_P\left[\sin\psi\sin\left(\omega t-\psi\right)+\left(\cos\psi-\frac{1}{2}\right)\cos\left(\omega t-\psi\right)\right] \quad ;\\
\frac{\phi_i}{N} &= \frac{v_B\, b}{2\cdot 10^8}H_P\left[\left(1-\cos\psi\right)\sin\left(\omega t-\psi\right)\right] \quad .
\end{aligned} \tag{B.3}$$

For a half winding over the poles at each end, referred to a method B we obtain:

$$
\begin{aligned}
\Phi &= -\frac{1}{2}\Phi_0\,\left[\cos(\omega t-\psi)-\cos\omega t\right] \quad ;\\
H &= -\frac{1}{2}H_P\,\sin(\omega t-\psi) \quad ;\\
J_f &= \frac{\sigma\, v_B}{2\cdot 10^8}H_P\left[\sin(\omega t-\psi)-\sin\omega t\right] \quad ;\\
J_t &= \frac{\sigma_t\, v_B}{2\cdot 10^8}H_P\left[\sin(\omega t-\psi)-\sin\omega t\right] \quad ;\\
\frac{\partial NI_m}{\partial z} &= \frac{5d}{2\lambda}H_P\cos(\omega t-\psi) \quad ;\\
\frac{\phi_i}{N} &= \frac{v_B\, b}{2\cdot 10^8}H_P\,\left[\sin(\omega t-\psi)-\sin\omega t\right] \quad .
\end{aligned}
\tag{B.4}
$$

The output power P_0 and the power losses P_{Ohm} and P_t for the two methods of end grading are given in table B1, where for convenience these quantities are expressed as ratios of the corresponding quantities for the ideal case

	End grading Method A	End grading Method A
	Sum of inlet and outlet graded region	
$k_{oe}=\frac{P_0}{P_\lambda}(1-s)s$	$\frac{1}{8}\left(3-\frac{1-s}{s}\right)$	$\frac{1}{4}$
$k_{fe}=\frac{P_f}{P_\lambda}s^2$	$\frac{1}{8}\left[3+\left(\frac{1-s}{s}\right)^2\right]$	$\left(\frac{1+s^2}{4s^2}\right)$
$k_{te}=\frac{P_t}{k_{t1}}P_\lambda$	$\frac{3}{8}$	$\frac{1}{2}$
	Total for pump of *n* pole pairs* or wavelengths, including mid and end graded regions	
$k_o=\frac{P_0}{P_\lambda}(1-s)s$	$n-1+\frac{1}{8}\left[3-\left(\frac{1-s}{s}\right)\right]$	$n-1+\frac{1}{4}$
$k_f=\frac{P_f}{P_\lambda}s^2$	$n-1+\frac{1}{8}\left[3+\left(\frac{1-s}{s}\right)^2\right]$	$n-1+\left(\frac{1+s^2}{4s^2}\right)$
$k_{t2}=\frac{P_t}{k_{t1}}P_\lambda$	$n-1+\frac{3}{8}$	$n-1+\frac{1}{2}$

Table B1: Gross output power and losses for the two possible methods of end grading. * The number of pole pairs *n* need not necessarily be an integer. Moreover, *n* includes the poles in the graded regions.

Physical units and variables

Small captions

Description	Symbol	Unit
Liquid metal gap	a	m
mean circumferrential extension of the duct	b	m
Specific heat capacity	c_P	$J/(kgK)$
Inner diameter of flow channel	d_i	m
Outer diameter of flow channel	d_a	m
Mean diameter of flow channel	d_m	m
Dimensions	dx, dy, dz	m
Frequency of power supply	f	$1/s$
Loss factor of pulsating filed	h	-
Electric current density	j	A/m^2
Fluid current density	j_f	A/m^2
Tube current density	j_t	A/m^2
Winding distribution factor	k_d	-
Tube loss power factor	k_{tl}	-
length of coil winding	l_{coil}	m
Number of phases	m	-
Pressure	p	N/m^2
Slip ratio	s	
Mean magnetic field velocity	v_B	m/s
Mean fluid velocity	v_f	m/s
Time	t	s

Large captions

Description	Symbol	Unit
Current carrying coil cross section	A_{coil}	m^2
Maximum magnetic field	B_{max}	T
Magnetic induction in passive core	B_C	T
Winding fill factor	F	-
Magnetic induction	H	T
Peak magnetic induction	H_P	T
Hartmann number	Ha	
Current	I	A
Current in the winding	I_m	A
Current in the wall	I_T	A
Supply current per length	J	A/m
Effective pump length	L	m
Flux form factor	M	-
Number of current turns	N	-
Flux form factor	N_1	-
Ohmic heating in coils	P_{Coil}	W
Hydraulic friction loss	P_{hydr}	W
Losses in iron sheets	P_{iron}	W
Ohmic loss in the fluid	P_{Ohm}	W
Total power input	P_{input}	W
Losses in the tube walls	P_{tube}	W
Viscous losses in pump channel	$P_{viscous}$	W
Winding loss	P_W	W
Gross output power	P_0	W
Power factor	P_λ	W
Flow rate	Q	m^3/h
Ohmic Resistance of the tube	R_t	Ω
Ohmic Resistance of the windings	R_{Wind}	Ω
Reynolds number	Re	-
Stewart number or interaction parameter	St	-
operation temperature	T_{op}	$°C$
Impedance of the coils	Z	Ω

Greek letters

Description	Symbol	Unit
Air gap core inductor	δ_{air}	m
Wall thickness inductor	δ_t	m
Wall thickness core	δ_t	m
electric potential	ϕ	V
Induced voltage per current turn	ϕ_i	V
Phase angle between flux and current	γ	
Effective real efficiency	η	$\%$
Ideal efficiency	η_t	$\%$
Overall Pump-efficiency	η_{tot}	$\%$
Phase shift voltage current	φ	°
Wave length	λ	m
Heat conductivity of the fluid	λ_f	$W/(mK)$
Heat conductivity of the wall	λ_t	$W/(mK)$
Magnetic permeability	μ	-
Magnetic permeability of vacuum	μ_0	$As/(Vm)$
Kinematic viscosity	ν	m^2/s
Fluid density	ρ	kg/m^3
Specific electric conductivity fluid	σ	$A/(Vm)$
Specific electric conductivity wall (tube)	σ_t	$A/(Vm)$
Rotation frequency	ω	s^{-1}
Hydraulic loss factor by Blasius	ξ_F	-
Hydraulic in- outlet loss factor	$\xi_{i,o}$	-
Phase angle	ψ	°
Pulsation loss factor	ζ	-
Magnetic flux	Φ	Tm^2

Figure Captions

Fig. 1.1: Schematic figure of the MEGAPIE design to be set-up at the PSI in Switzerland.

Fig. 2.1: Sketch of the operation principle of an electromagnetic induction pump on the basis of a cylindrical pump (ALIP).

Fig. 2.2: Terminology of the parts being used in an ALIP. Sketch of the generation of the magnetic flux by the windings and a list of the losses appearing in an electromagnetic pump.

Fig. 3.1: Principle sketch of the Tandem pump being developed at the Institute for Physics IP in Riga.

Fig.4.1: Calculated effective efficiency η of an asynchronous machine as a function of the slip s.

Fig. 5.1: Coordinate system and quantities being used in the pump analysis.

Fig. 5.2: General arrangement and quantities involved in the analysis of a linear induction pump.

Fig. 5.3: Electric current density J in $[A/m]$ required to attain the desired pressure head as a function of the wavelength λ for the main pump (a) and the bypass pump of the Riga tandem pump.

Fig. 6.1: Location of temperature sensors proposed for the main pump of the Riga tandem pump.

Fig. 7.1: Velocity (——) and magnetic field (- - -) distribution as a function of the radius at the end of the main pump.

Fig. 8.1: Technical sketch of the main pump of the Riga tandem unit. (a) Iron package consisting of 678 steel sheets. (b) extension of the ferromagnetic iron package. (c) Coil system and its connectors. (d) cross sectional cut through one coil package and wire dimensions. (e) Inner core inductor and its dimensions.

Fig. 8.2: Technical sketch of the bypass pump of the Riga tandem unit. (a) Inductor and inner core, Iron package consisting of 1068 steel sheets. (b) Coil system and its connectors. (c) cross sectional cut through one coil package (wire dimensions are the same as in the main pump).

Fig.8.3: Attainable pressure head Δp in bar and related flow rates Q in m^3/h of the main pump (a) and the bypass pump (b) as a function of the supplied current I in $Ampere$.